

Final Technical Report

AFOSR Grant F49620-93-1-0220

Research on X-ray Nonlinear Optics and Single-Particle Applications

Department of Electrical and Computer Engineering
The Johns Hopkins University, Baltimore, MD 21218

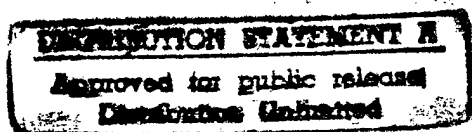
Submitted to

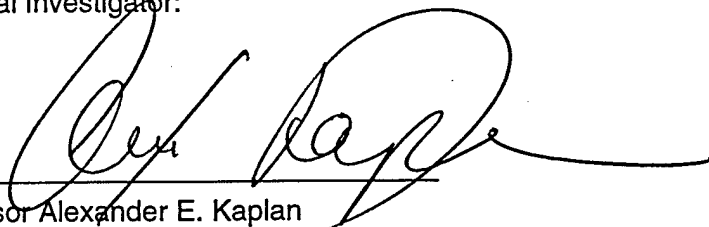
the U.S. Air Force Office of Scientific Research
Program Manager - Dr. Howard Schlossberg

Baltimore, Maryland
April 1997

Project Period: March 1, 1993 - February 28, 1996
(no-cost extension March 1, 1996 -- February 28, 1997)

Principal Investigator:





Professor Alexander E. Kaplan
ph. (410) 516-7018
FAX (410) 516-5566
e-mail sasha@super.ece.jhu.edu

19970506 045

DTIC QUALITY INSPECTED 3

Table of Contents

	Page
1. Brief overview of technical results	3
2. Technical Reports on Specific Projects	4
2.i. Research on X-ray nonlinear optics	4
2.i.1. Resonant frequency transformations of short-wavelength coherent radiation in plasma	5
2.i.2. Multiphoton processes in X-ray domain	6
2.i.3. X-ray stimulated electronic Raman scattering in non-ionized gases	7
2.ii. Phase-matching optimization of large-scale nonlinear frequency upconversion in neutral and ionized gases	8
2.ii.1. Optimal quasi-phase-matching for high-order harmonic generation in gases and plasma	9
2.ii.2. Large-scale nonlinear frequency upconversion by high-order difference-frequency mixing.....	10
2.ii.3. Phase-matching optima beyond perturbation limit.....	11
2.iii. Super-dressed two-level atom: very high harmonic generation and multi-resonances.....	12
2.iv. Modulation-induced inhibition of dynamics and high-order frequency mixing	13
2.v. Bright-bright 2π -solitons in stimulated Raman scattering	14
2.vi. Non-oscillating high-intensity subfemtosecond solitons.....	15
2.vi.1. Subfemtosecond pulses in mode-locked 2π -solitons of the cascade stimulated Raman scattering	17
2.vi.2. "Electromagnetic bubbles"	18
2.vii. Two-photon induced fluorescence of biological markers using optical fibers.....	19
2.viii. Other research	19
2.viii.1. Eigenmodes of $\chi^{(2)}$ wave-mixings: cross-induced 2-nd order nonlinear refraction	19
2.viii.2. X-ray narrow-line transition radiation source based on low-energy electron beams traversing a multilayer nanostructure	20
3. Work published under AFOSR grant F49620-93-1-0220	23

1. Brief overview of technical results

The AFOSR grant F49620-93-1-0220 was activated on March 1, 1993 with the project period of three years ending on February 29, 1996. The research of this principal investigator has been supported by AFOSR continuously for 17 years by now. During this period, under AFOSR support, the principal investigator authored or coauthored about 250 publications, among them about 10 book contributions, 80 regular journal papers, one patent, and 26 conference proceedings papers; the rest are conference papers.

Under the AFOSR grant F49620-93-1-0220, 60 new papers have been published by this principal investigator and his group, among them 19 papers in regular journals [1-19], 2 book contributions [20,21], 10 conference proceedings papers [22-31], and the rest are conference papers [32-60].

Most of the effects proposed under the AFOSR support are novel and have initiated new opportunities in the field. The work by this PI is highly credited by the research community in the field. Within the last five years, for example, his work was cited for about 400 times (according to "Science Citation Index ") by other researchers. He has been a member of program committees and a panel member of several technical conferences on nonlinear optics and quantum electronics, and an editorial board member of the "International Journal of Non-linear Optical Physics and Materials".

Under AFOSR grant F49620-93-1-0220, a number of new results were obtained by this principal investigator and his group in the field of nonlinear optics and quantum electronics:

- i. Pioneering theoretical research on X-ray nonlinear optics, aimed to diversify coherent X-ray sources by means of nonlinear frequency transformations (mixing of X-ray and optical radiation, stimulated Raman scattering, etc.)
- ii. Theoretical research on phase-matching optimization of large-scale nonlinear frequency upconversion, with a potential to substantially improve the efficiency of this new source of short-wavelength coherent radiation.
- iii. Theory of high-harmonic generation in super-dressed two-level atoms.
- iv. Theory of modulation-induced inhibition of dynamics and high-order frequency mixing in two-level atoms.
- v. Bright-bright 2π -Solitons in stimulated Raman scattering.
- vi. Pilot theoretical research on the subfemtosecond soliton formation and propagation, in particular, on subfemtosecond pulses in mode-locked 2π -solitons of the cascade stimulated Raman scattering, and the so called electromagnetic bubbles.
- vii. Experimental research on biological applications of nonlinear laser spectroscopy (two-photon induced fluorescence).

- viii. Other research: eigenmodes of $\chi^{(2)}$ wave-mixings and X-ray narrow-line transition radiation source based on low-energy electron beams traversing a multilayer nanostructure.

2. Technical reports on specific projects

2.i. Research on X-ray nonlinear optics

[5,7,8,20,22,25,27,29,30,31,32,36,46,47]

Recent years have witnessed a steady progress in X-ray laser (XRL) research: several XRLs near 200 Å demonstrated saturation and high degree of spatial coherency, with the output of ~ 1 MW; the Y XRL at LLNL attained very high output of ~ 40 MW; mirrors and polarizers were developed; cavity operation and cascade X-ray amplification were tried; and some promising steps to table-top X-ray lasers were made.

At the same time, XRL applications are still in the very early stages, being limited essentially to Y XRL interferometry of plasma for ICF research and a few experiments with X-ray microscopy. The relatively high cost of existing XRLs is not the main obstacle to their applications, since even XRLs already developed could be much less expensive if realized on specialized equipment, not to mention using them as national facilities. More important is that XRL applications to spectroscopy, microscopy, and technology would require large variety of sources, especially at high frequencies, and availability of tunable coherent X-rays. At longer wavelengths (IR, visible, UV), coherent radiation sources are diversified largely by nonlinear optical transformations. In X-ray domain, due to very limited number of XRLs with substantial output (out of ~ 50 reported X-ray laser lines less than 10 demonstrate high output), At the same time, the output power of some XRLs is comparable to the Q-switched output of optical lasers and seems to be high enough for efficient nonlinear transformations in highly-resonant nonlinear media.

Using a theoretical base created by us under the previous AFORS grants, we have theoretically explored, under current AFOSR support, a large variety of nonlinear frequency transformations with potentially high conversion efficiency [20,22,27,29,30,31,32,46,47]. We have also considered in detail X-ray stimulated Raman scattering in gases and vapors [5,7,8,25,36], which renders the first relatively efficient X-ray frequency transformation in non-ionized media ever proposed. Finally, we did a pilot research on the feasibility of multiphoton processes in X-ray domain, which could open a way to generating coherent radiation at very short (of a few Å) wavelengths [30].

2.i.1. Resonant frequency transformations of short-wavelength coherent radiation in plasma [20,22,27,29,30,31,32,46,47]

Recently, a few theoretical papers on the feasibility of soft-X-ray laser frequency upconversion in plasma have been published by us and other researchers. In these papers, XRL frequency tripling, $\omega = 3\omega_{XRL}$, and near-doubling, $\omega = 2\omega_{XRL} - \omega_{opt}$ have been considered. (Here ω_{XRL} and ω_{opt} are frequencies of an XRL and a longer-wavelength laser, respectively; since $\omega_{opt} \ll \omega_{XRL}$, $\omega \sim 2\omega_{XRL}$ in the latter process.) It has been shown, in particular [33], that conversion efficiency C_{eff} of the X-ray frequency near-doubling might in some cases be comparable to the conversion efficiency in visible domain, due to good multiple-resonant conditions and the participation of very powerful longer-wavelength lasers.

In this research, we have identified and estimated multiple-resonant plasma media for efficient frequency transformation of X-ray and an XUV laser radiation by a larger variety of four-wave mixing (FWM) processes. Our estimations show that high conversion efficiency is attainable with available short-wavelength output and contemporary plasma and X-ray optics technology. If realized experimentally, these nonlinear transformations may result in new X-ray coherent sources, including generation of coherent radiation at wavelengths as short as 22 Å, and in both "line-by-line" and continuously tunable X-ray lasing.

In the course of our research we have considered generation of about 30 new soft-X-ray lines. In addition to XRL frequency near-doubling [5], the following frequency transformations are expected to be among the most efficient [22,32] (see Fig. 1):

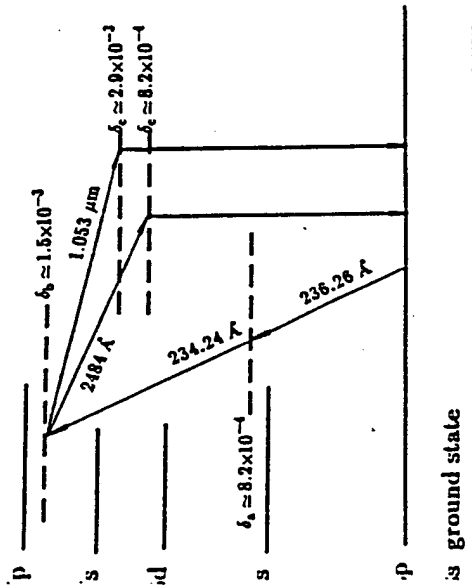
(i) **Difference-frequency mixing (2) of Ge XRL 232.24 Å and 236.26 Å with either Nd or KrF laser radiation in Na-like Ar** (Fig. 1a). Very high conversion efficiency is expected at both 118.43 Å (with Nd laser) and 122.91 Å (with KrF laser) output wavelengths, due to excellent resonances. Note that the 122.91 Å pulse would be as short as KrF laser pulses are, that is, possibly < 1 ps. In collaboration with Prof. M. H. Key of Rutherford Appleton Lab, UK, we have considered a proof-of-principle experiment on DFM of Ge XRL developed in the UK [27].

(ii) **Frequency shift of Y²⁹⁺ 155 Å or Se²⁴⁺ 206.38 Å line by mixing with two optical lines** (process $\omega = \omega_{XRL} + \omega_{opt_1} - \omega_{opt_2}$) (Fig. 1b). In both cases, the two optical lines are the fundamental and the second harmonics of the same Nd laser. Efficiency of a few tens of percent is expected for conversion of both Y (152.73 Å output) and Se (205.71 Å output) lines.

(iii) **Cascades of highly-resonant difference-frequency mixing processes of X-ray and optical radiation.** Such processes may provide a bridge between powerful Y, Se and Ge XRLs and the "water window" (radiation with wavelength between ~43 Å and ~25 Å believed to be the best for X-ray microscopy of living cells), with possible total photon conversion efficiency of a few percent. In one of the possible cascades (see Fig. 1c), mixing of two photons of Se XRL 209 Å line with one Nd laser photon in K IX yields 107 Å output. At the next step, mixing of two 107 Å photons with another Nd laser photon in Ti XII yields 53.77 Å radiation. Eventually, mixing of 53.77 Å, 206 Å, and Nd radiation in Zn XX produces 43 Å output.

Difference-frequency mixing:
Ge²⁴⁺ lines in Na-like Ar VIII with:

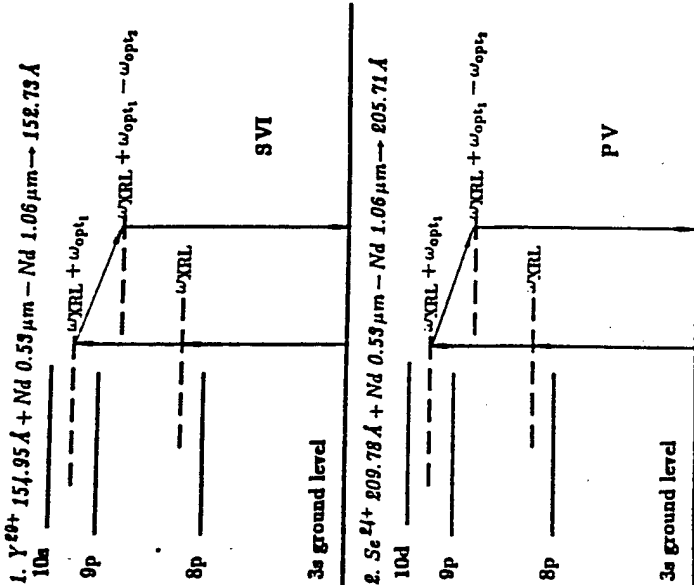
Nd 1.053 μm \rightarrow 118.43 \AA
KrF 2484 \AA \rightarrow 122.91 \AA



$C_{eff} \sim 1$ for optical laser power $\sim 10^{10}$ W

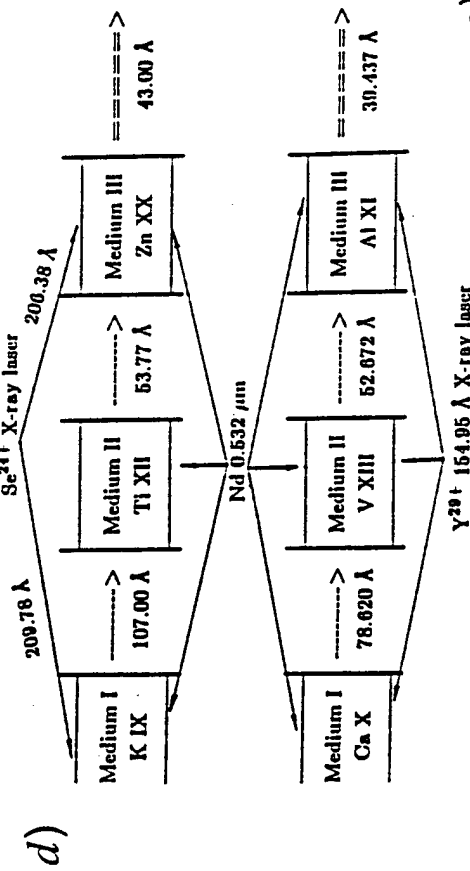
a)

XRL frequency shift: FWM with two optical lasers



b)

Cascades of difference-frequency mixing: towards "water window"

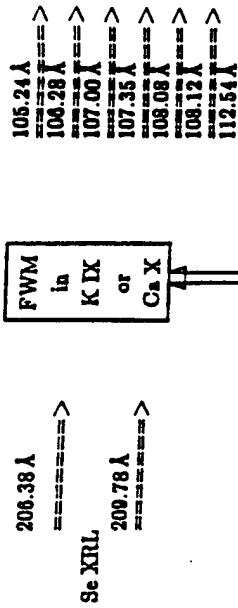


d)

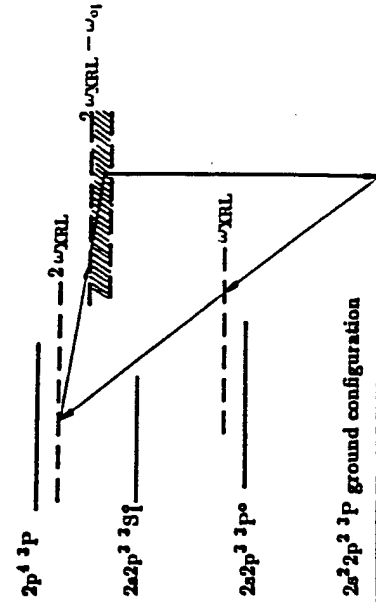
Fig. 1. Frequency transformations of X-ray laser radiation.

X-ray laser tunability

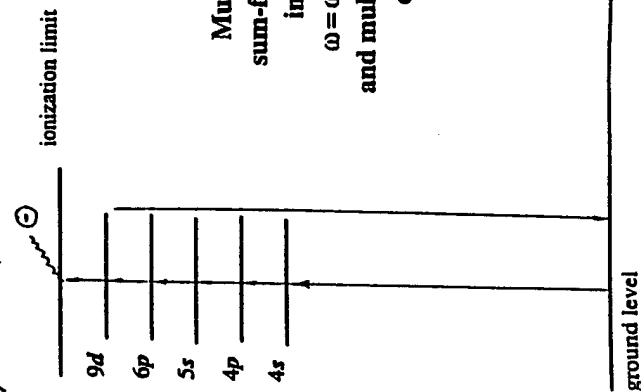
1. "Line-by-line" tunability: FWM with optical lines



2. Continuous tunability: FWM with tunable lasers



c)



e)

(iv) **Tunable coherent X-rays** can also be generated by difference-frequency mixing of coherent X-ray and optical radiation (see Fig. 1d). By mixing of the two Se XRL lines with the lowest harmonics of Nd or KrF lasers in K IX or Ca X, one may attain "line-by-line" tunability near 107 Å with high C_{eff} (possible output at 105.24 Å, 106.28 Å, 107.00 Å, 107.35 Å, 108.08 Å, 108.12 Å, and 112.54 Å). Continuous tunability can also be achieved by FWM, now with a tunable longer-wavelength laser, similarly to generation of tunable VUV radiation. In soft-X-ray domain, however, both two- and one-photon resonances are necessary for a reasonable conversion efficiency. C-like ions may provide suitable media for this process. Expected conversion efficiency is of order of 10^{-5} for MW X-ray pumping and GW optical pumping.

2.i.2 Multiphoton processes in X-ray domain [30]

Multiphoton interactions of optical lasers with gases and plasma such as multiphoton ionization, which is now an important new area of atomic physics, or high-harmonic generation (HHG), a strong manifestation of nonperturbative nonlinear optics and an important new source of short-wavelength coherent radiation, have recently attracted much attention. We believe that parameters of existing X-ray lasers are already close to those required for observing similar multiphoton effects at much shorter wavelength, with similar potential impact on physics of highly-ionized atoms and X-ray nonlinear optics. As usual, the easiest to observe are resonantly enhanced processes. For instance, multiphoton absorption $\omega_{C^{5+}XRL} + 4\omega_{4673\text{\AA}}$ in Ne-like Mg (see Fig. 1e) would be resonantly enhanced at each step so that very strong excitation and ionization of Mg^{2+} to F-like stage would take place even at modest C^{5+} XRL intensity. In the same media, strong multiphoton absorption is expected for Ge XRL + optical pumping.

On the other hand, high-order harmonic generation is a non-resonant process, which requires high-intensity lasers even at longer wavelengths and, therefore, may seem to be totally out of reach for X-ray lasers. Yet, our estimates based on our two-level model of HHG [4,24,28,29] allowed us to suggest X-ray HHG at already available XRL output power (provided that a substantial improvement in the beam quality is attained in the experiment). Indeed, the most obvious manifestation of HHG is the presence of the "plateau": the intensities of generated harmonics are approximately the same within a large range of harmonics numbers. Our model [4] approximates a rare gas atom in HHG by a two-level atom and yields for the critical intensity I_{cr} , i. e. the pumping intensity necessary for the plateau formation: $I_{cr} \sim |d|^2/\omega_0 \omega$, where ω_0 and $|d|$ are the transition frequency and the dipole moment of the model two-level system, respectively, and ω is the frequency of the pumping laser. If one assumes that $|d| \sim \omega_0^{-1/2}$, then I_{cr} scales as ω_3 , provided the ratio of the pumping frequency ω to the ionization potential of the medium remains constant. In particular, it follows from the critical intensity being approximately equal to $2 \times 10^{13} \text{ W/cm}^2$ for HHG of an 616 nm laser in neutral argon [37] that the Y^{29+} XRL intensity of about $1.3 \times 10^{18} \text{ W/cm}^2$ might be enough to observe X-ray HHG in Ar-like Kr. Such intensity would be attainable with the available Y XRL power of $\sim 40 \text{ MW}$ if it becomes possible to focus the beam to e. g. three times diffraction-limited spot of

$\sim 3\lambda$. Moreover, a few times larger intensity might generate a fully developed plateau such that the 21st harmonic (7.4\AA) would be as intense as the 5th harmonic.

2.i.3 X-ray stimulated electronic Raman scattering in non-ionized gases [5,7,8,25,36]

The vast majority of all the media proposed for X-ray resonant nonlinear optics have been plasmas. The feasibility of X-ray nonlinear effects in non-ionized materials, interesting theoretically and important experimentally (since it is much easier to work with neutrals), depends on whether resonances to XRL lines exist in neutral atoms, and whether the processes of interest would have time to develop before the medium becomes totally ionized by intense X-rays. We proposed for the first time two schemes for observing a resonant X-ray nonlinear effect, stimulated electronic Raman scattering (SERS), in non-ionized media -- He and Li vapor, and showed that very high conversion efficiencies may be achieved by operating in high pump energy regime in which total ionization of the media occurs in a time period much shorter than the pulse duration. We have studied in detail the dynamics of the process and predicted soliton-like pulses and precursors at the Stokes frequency at the photoionization front of pumping X-ray radiation [7].

X-ray SERS could be observed only if resonantly enhanced by tuning the pumping frequency close to some transition from the initial Raman level. Since X-ray laser photon energy (50-300 eV) is much larger than the binding energy of optical electrons in all the neutral atoms, we propose making use of so called core-excited atomic states. In particular, some double-excited levels of He and Li atoms are resonant to the powerful Se^{+24} 20.9 nm X-ray laser. Two transition schemes were considered (see Fig. 2): (i) He: $1\ ^1S \rightarrow 2s2p\ ^1P \rightarrow 2\ ^1S$ (the Stokes wavelength 32.2 nm), and (ii) Li: $1s^22s \rightarrow [1s(2s2p)\ ^1P]^2P \rightarrow 1s^23s^2S$ (the Stokes wavelength 22.3 nm). Our estimates of small-signal gain have shown that significant Stokes output requires pump intensity of the order of $10^{12} - 10^{14}\text{ W/cm}^2$, which is readily available; it would, however, fully ionize a medium within a fraction of the Se XRL pulse duration. Thus, effective Stokes generation can take place only at the leading edge of the laser pulse, before the full ionization sets in.

Fig. 3 depicts typical numerical solutions of Maxwell-Bloch equations for X-ray SERS in Li; normalized Stokes pulse energy flux is shown as a function of the cell length z for $N=10^{18}\text{ cm}^{-3}$. One can see two distinct stages of this Raman process, the exponential growth and the saturation. In the exponential region the Stokes pulse width is constant and its peak coincides with the leading edge of the pump pulse whose velocity is limited by the photoionization to be smaller than c . In the saturation region, the Stokes pulse intensity is almost constant while the pulse width increases linearly with the distance z . An approximate analytical model developed by us, in particular, yielded an estimate of the optimal length of the Raman medium; e. g., for the attainable XRL pulse energy of $300\ \mu\text{J}$, the optimal focusing for $N=10^{18}\text{ cm}^{-3}$ is $b=L \approx 5.65\text{ cm}$, and the total exponential gain at the cell end is $GL \approx 23$, L being the length of

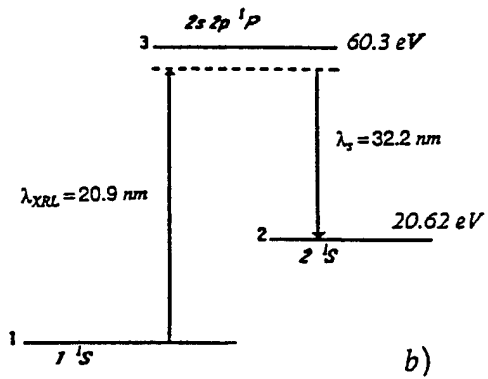
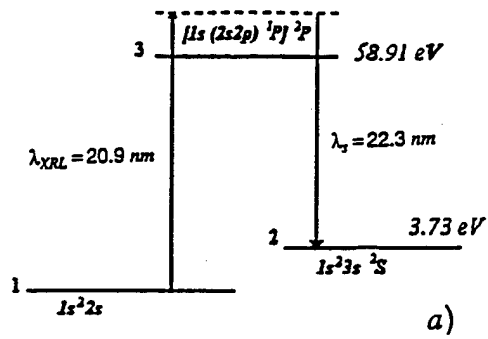


Fig. 2 X-ray Raman transitions in a) Li and b) He, resonant to Se XRL radiation.

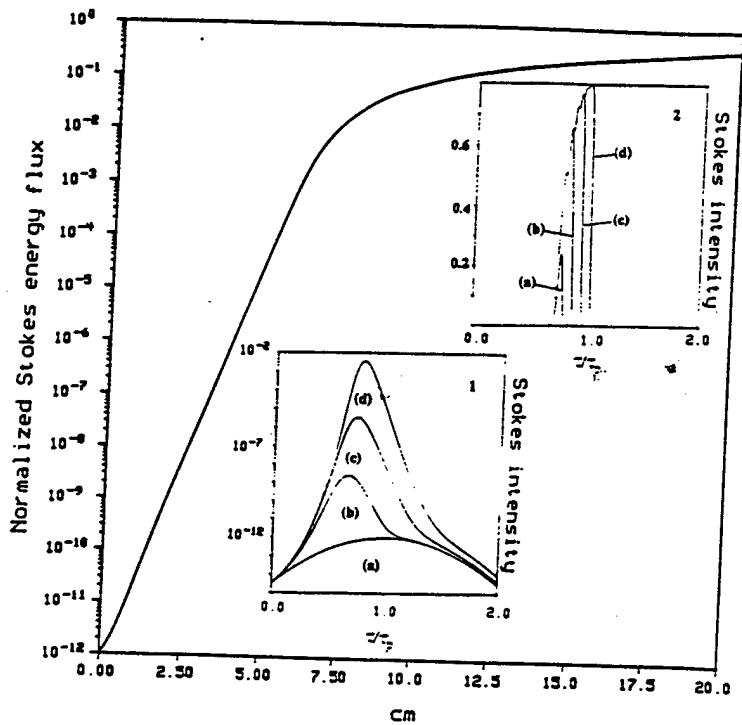


Fig. 3 Normalized Stokes energy flux $J_s(z)/J_p$ in Li as a function of the cell length z . Insets: Normalized Stokes intensity $I_s(z, \tau)/I_{p_{max}}$ as a function of normalized retarded time τ/τ_p in (a) exponential region; curves: 1 - $z=0$ cm; 2 - $z=2$ cm; 3 - $z=4$ cm; 4 - $z=6$ cm; in (b) linear region; curves: 1 - $z=8$ cm; 2 - $z=12$ cm; 3 - $z=16$ cm; 4 - $z=20$ cm.

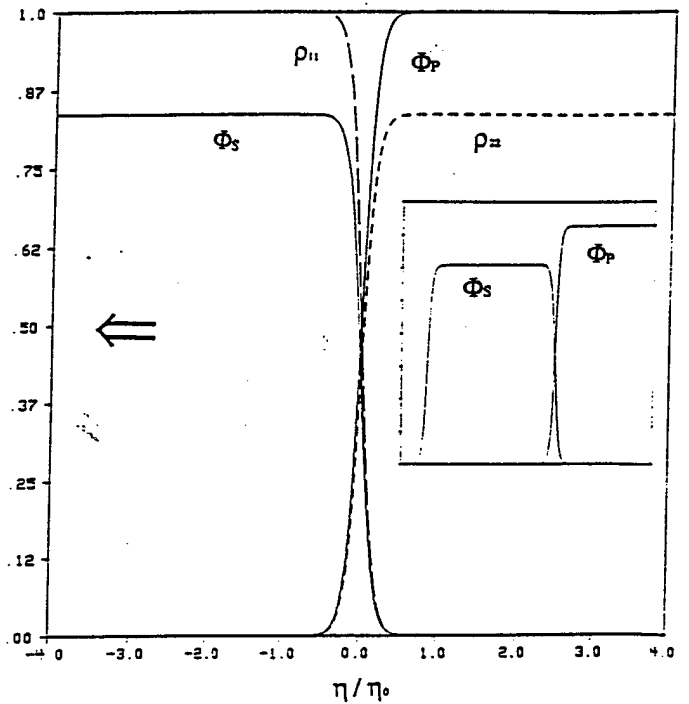


Fig. 4 The pump, Φ_p , and Stokes, Φ_s , photon fluxes (normalized to $\Phi_p(\infty)=\Phi_0$), and the population of the ground, ρ_{11} , and excited, ρ_{22} , levels as a function of the normalized retarded time η/η_0 for IFSR soliton in He (for η_0 see in the text). The arrow indicates the direction of the pulse propagation.

the medium.

One of our major results is the finding that X-ray SERS can significantly inhibit the photoionization of the media and lead to formation of soliton-like pulses and precursors at the Stokes frequencies. Numerical solution for the intensities and populations for SERS in He (Fig. 4) shows that the coherent SERS significantly inhibits the photoionization of neutral atoms by X-ray radiation. This inhibition is due to the fact that a significant portion of neutral atoms ends up being "parked" at the upper excited level, whose photoionization cross section is very small. As a result, "ionization-front stimulated Raman" (IFSR) soliton is formed: while the trailing edge of the Stokes pulse travels with the same velocity as the photoionization front, its leading edge travels much faster, with the velocity of light in the neutral media. The length of such an almost rectangular pulse increases linearly with the distance traveled in media [5]. Therefore, in the X-ray IFSR soliton we have a strong "Stokes precursor", arriving at the end of the cell significantly ahead of pumping, which can be used for measurements, and for "pilot warning" of the trailing photoionization front. For propagating distance of 10 cm in *Li*, pump intensity of 10^{12} W/cm^2 and $N = 10^{18} \text{ cm}^{-3}$ ($\sim 0.1 \text{ atm}$ at $T=800\text{K}$) the "warning time" is $\sim 100 \text{ ps}$.

2.ii. Phase-matching optimization of large-scale nonlinear frequency upconversion in neutral and ionized gases [2,10,11,18,24,28,33,42,45,48]

Bright, short-wavelength ($\lambda < 1000 \text{ \AA}$), coherent radiation would find numerous applications in areas as different as cell biology and material science. High-harmonic generation (HHG), $\omega_q = q \omega$, of optical and UV lasers in gas jets has succeeded in generating harmonics of a Nd:YAG laser ($\lambda \sim 1 \text{ }\mu\text{m}$) at wavelength as short as 7.6 nm. The harmonic energy is, however, severely limited by very low conversion efficiency (defined as the ratio of harmonic power to the incident power); as a result, noticeable output requires very high pumping energy. Such low efficiency (below 10^{-7} for the highest to date applied power) is to a large extent due to poor phase matching. If phase-matched, HHG of widely available short-pulse high-intensity lasers could become a convenient, in principle table-top source of coherent, easily tunable short-wavelength radiation. Current experimental conditions of HHG are, however, very far from optimal, phase-matching-wise: the strong positive dispersion of even slightly ionized media requires, for the experimental design used, very loose focusing of the pumping beam, and, therefore, very high pumping energy. A similar problem has been successfully dealt with in third-harmonic generation (THG). Some approaches developed for THG and discussed recently in application to HHG, however, either would be of no help for very high-order harmonics, like using resonant refraction, or would yield phase matching factors many orders of magnitude lower than optimal, like using semi-infinite media.

In this research, we have proposed [2,10,11,18,24,28,33,42,45,48] two techniques that could improve radically the efficiency of large-scale nonlinear frequency upconversion: quasi-phase-matching of high-order harmonic generation in density-modulated media, and using

high-order difference-frequency mixing in plasma. The most important advantage of the proposed methods is that both techniques allow for optimal phase matching with tight focusing of pumping beams, which is detrimental for current approaches to frequency upconversion, with potential increase in conversion efficiency by several orders of magnitude. Optimal phase-matching conditions obtained by us in the perturbation limit are likely to hold for strong (stronger than atomic field) pumping fields as well [10,15,28].

2.ii.1. Optimal quasi-phase-matching for high-order harmonic generation in gases and plasma [11,18,45,48]

Recently, plasma density modulation has been proposed as a method to optimize phase matching for THG by relativistic plasma electrons. This idea is essentially a ramification of the well known method of quasi-phase-matching (QPM) proposed first in 1962 and extensively studied in the following years -- but almost exclusively for the second-harmonic generation in solids. This lack of interest in QPM in higher-order harmonic generation is, most likely, due to the existence of potentially much better and less cumbersome methods to optimize THG phase matching. Many phase-matching techniques successful in THG are, however, of much less use for HHG, which makes QPM more attractive.

In this research, we have theoretically demonstrated the feasibility and potentials of QPM optimization of HHG by a focused beam in plasma or a gas whose nonlinear susceptibility and refractive index are spatially modulated, in particular through the medium density modulation. In order to obtain analytic results, we rely on the perturbation-theory expressions for the phase-matching factor; our results remain valid beyond perturbation limits as well, if some general assumptions hold regarding nonlinear polarization induced by strong laser field (see 2.ii.3).

We assume that the medium density modulated along the beam propagation axes z in such a way that the refractive index can be written as $n(u) = 1 + \tilde{n} [1 + A \cos(au)] = n_0 + \tilde{n} A \cos(au)$, where $u = 2z/b$, $n_0 = 1 + \tilde{n}$ is the ambient refractive index, \tilde{n} is proportional to the ambient medium density; and the nonlinear susceptibility responsible for the q th harmonic generation, $\chi^{(q)}$, is spatially modulated as $\chi^{(q)}(u) = \chi_0^{(q)} [1 + A \cos(au)]$, $a = \pi b/\lambda_m$, where λ_m and $A < 1$ are the modulation wavelength and amplitude, respectively, $\chi_0^{(q)}$ is the ambient (unperturbed) nonlinear susceptibility. Then, if a beam is tightly focused ($b \ll L$) to a small confocal parameter in a not too dense plasma, or in a neutral gas, then optimal modulation wavelength is $\lambda_m^{opt} \approx \pi b/(q-2)$. As an illustration, consider QPM for the 51st harmonic of a Ti:Sapph laser ($\lambda = 0.8 \mu m$), which is near the middle of the harmonic plateau in the recent HHG experiments, and assume $b = 100 \mu m$. Then, $\lambda_m^{opt} \approx 6.2 \mu m$ in plasma with $N_e \sim 10^{18} cm^{-3}$.

An important advantage of QPM optimization is that it allows for tight focusing otherwise detrimental for HHG in rare gases and plasma. The incident intensity could then be easily increased by two orders of magnitude for the same pumping power by e. g. simply changing

the confocal parameter from $\sim 1 \text{ mm}$ used now, to readily attainable $100 \mu\text{m}$. Without a general theory of phase matching beyond perturbation limits, or at least numerical simulations for a particular laser and a medium, it is impossible to calculate accurately the resulting increase in harmonic intensity. It is commonly assumed, however, that the intensity of high-order harmonics is approximately proportional to the 12th power of the incident intensity. Moreover, even for the currently used incident intensity, QPM optimization may significantly increase HHG conversion efficiency. Our estimates show that with recently reported plasma density modulation done by irradiating a grating with a ruby laser ($A \approx 0.08$, $\lambda_m \approx 2-6 \mu\text{m}$ in a plasma with $N_e \sim 10^{18} \text{ cm}^{-3}$), QPM optimization might increase the harmonic intensity by a factor of ≈ 160 for the same pumping intensity.

2.ii.2. Large-scale nonlinear frequency upconversion by high-order difference-frequency mixing [2,10,18,24,28,33,42,45,48]

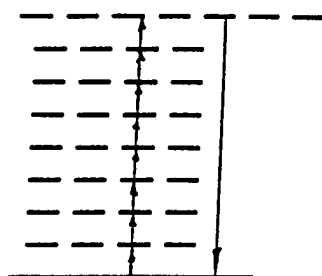
Even QPM, potentially the most promising method of HHG phase matching, would yield the phase-matching factor two orders of magnitude smaller than the factor attainable in media with negative dispersion. In other words, plasma remains an inherently hostile medium for harmonic generation, as far as phase matching is concerned. At the same time, substantial presence of free electrons at high laser intensities is practically unavoidable; moreover, theoretical models and recent experimental results suggest that HHG in ions would yield substantial output at much shorter wavelength than HHG in neutral atoms. It would be, therefore, much more advantageous not to fight an uphill battle with plasma dispersion, but use it as an ally. The need in such an ally is obvious from the necessity to compensate for large geometrical mismatch by large dispersion. Plasma dispersion is large; unfortunately, for HHG its sign is "wrong" (see Fig. 5). What we have proposed is using for large-scale nonlinear upconversion, instead of HHG, another nonlinear effect, *high-order difference-frequency mixing* (HDM) in plasma. HDM is the process of generating coherent radiation at the frequency ω , $\omega = m\omega_1 - l\omega_2$, (m and l are integers, $m \gg 1$) when laser beams with two substantially different frequencies ω_1 and ω_2 , interact in a nonlinear medium. We assume that $\omega_2 \ll \omega_1$ and $m > l$, so that shorter wavelengths could be attained by HDM of a given overall order $(m + l)$. In this Section, we demonstrate that HDM presents much better potentials for large-scale nonlinear upconversion of the frequency ω_1 than HHG, in that HDM allows *optimal* phase matching in ionized media. Indeed, in the absence of close resonances to both incident and generated radiation, Δk for HDM is determined by free-electron dispersion only and can be written for collinear beams as $\Delta k_{HDM} \approx r_e N_e m [\lambda_1 - (l/m)\lambda_2]$. Obviously, by choosing (or tuning) the second laser and/or changing plasma density and the confocal parameters, one can in principle adjust phase mismatch Δk to any sign and/or size of the optimal $b\Delta k$.

To transform these qualitative remarks into quantitative estimations of optimal media and laser parameters, we have generalized, to the mixings of arbitrary orders, the theory of phase matching developed in [48] for the third-order mixing. On the basis of derived by us analytical

Phase matching of high-order multiwave mixing in plasma

High-order harmonic generation (HHG)

$$\omega = q\omega_1$$



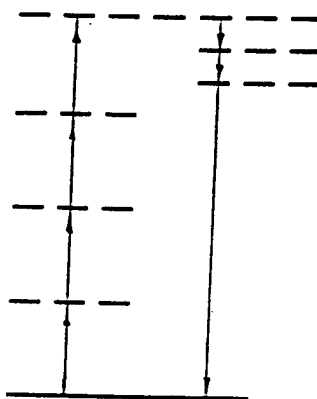
Plasma dispersion UNFAVORABLE:

- Optimal mismatch: $b\Delta k = -2(q-2) < 0$
- Plasma mismatch: $\Delta k = q r_e N_e \lambda_1 > 0$

High-order difference frequency mixing (HDM)

$$\omega = m\omega_1 - l\omega_2$$

$$m > l, \omega_2 \ll \omega_1$$



- Optimal phase mismatch $b\Delta k \approx -2(m-l-1) < 0$
- Plasma mismatch: $\Delta k \approx r_e N_e [m\lambda_1 - l\lambda_2]$ can be adjusted

In HDM:
Geometrical phase shift balanced by
large plasma dispersion
Tight focusing (= higher intensity) allowed

Fig. 5 Comparison of phase matching conditions for HHG and HDM in plasma.

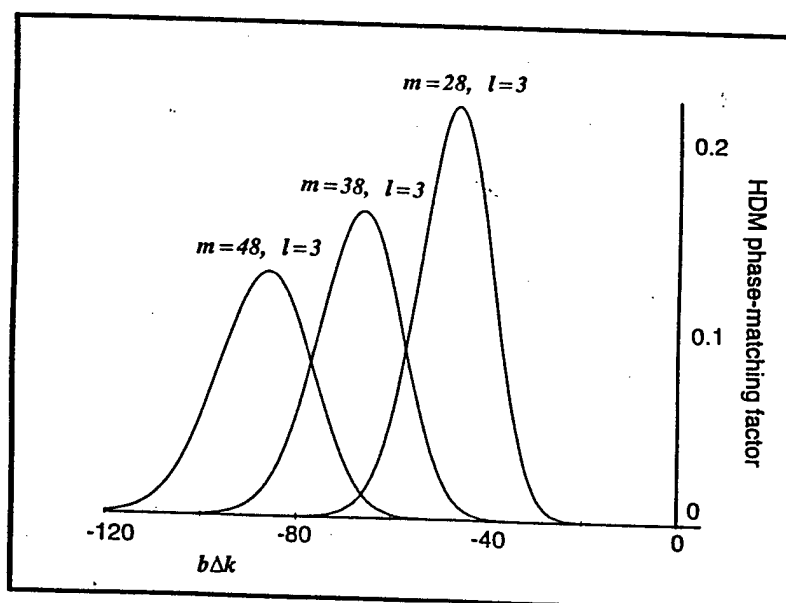


Fig. 6 Examples of HDM phase matching factors.

expressions for phase-matching factor that determines the HDM output for tightly focused collinear beams in homogeneous plasma, we have obtained an analytical approximation of optimal HDM phase matching conditions, $(b\Delta k)_{opt} \approx -2(m-l-1)$. Phase matching of a particular HDM process can be optimized as follows. For given m, l , one calculates $(b\Delta k)_{opt}$. Substituting the result into the expression for Δk_{HDM} , one obtains the relation between the confocal parameter and electron density required for optimal phase matching. Moreover, with phase-matching curves being quite broad (see Fig. 6), any given combination of N_e and b provides almost optimal phase matching not just for one but for a number of m, l sets.

A proof-of-principle experiment on HDM could utilize the fundamental and a harmonic of the same laser. To illustrate the numbers involved, let us consider HDM of the fourth ($\lambda_1 \approx 0.266 \mu m$) and the fundamental ($\lambda_2 \approx 1.064 \mu m$) harmonics of a Nd:YAG laser, with equal confocal parameters of 1 mm. Then, e. g., HDM with $l=5, m=18$ ($\lambda \approx 14.9$ nm) will be optimally phase matched in plasma with $N_e \approx 9 \times 10^{18} \text{ cm}^{-3}$. For $l=12, m=43$ ($\lambda \approx 7.8$ nm), the optimal plasma density is $\approx 1.6 \times 10^{19} \text{ cm}^{-3}$. A more promising, and more difficult, could be HDM of a harmonic and a Stokes wave of the same laser.

2.ii.3 Phase-matching optima beyond perturbation limit [10,18,28,45]

Our conclusions on the feasibility and usefulness of HDM and QPM are based on phase-matching optima conditions, which in turn rely eventually on the perturbation-theory analytical expression for the induced polarization as a function of pumping fields. It is not clear, therefore, whether these conditions hold beyond perturbation approximation. Unfortunately, the exact dependence of the induced harmonic polarization on strong pumping fields remains unknown. Moreover, while numerous models of the atomic response in strong-field HHG have appeared in recent years, no model calculations of the dipole moment induced by strong *biharmonic* pumping, have been published yet. It may seem, therefore, that there is no way of knowing to what extent, if any, phase-matching optimization conditions developed by us are applicable beyond perturbation limit. We have theoretically demonstrated, however, that the optimal phase-matching conditions for both HHG and HDM **do not depend**, to a large extent, on a particular form of the induced dipole moment, as long as some quite general assumptions are valid [10,15,30]. As a result, we expect the conditions for phase-matching optimization to remain largely intact in strong pumping fields.

For multiwave mixing of lowest-order Gaussian beams with the amplitudes \tilde{E}_1, \tilde{E}_2 which propagate along z-axis and focused at $z=0$ with the same confocal parameters, we assume that the Fourier component of the induced nonlinear polarization responsible for high-order difference-frequency mixing of strong fields is: $P_{m,l} = P_0(\tilde{E}_1, \tilde{E}_2) \exp(-i\phi)$, $P_0^* = P_0$. The space-dependent amplitude P_0 which is a real quantity $[E_1(R,u)]^m [E_2(R,u)]^l$ for weak fields, is still real in Eq. (45); and the *space-dependent* phase of the induced dipole moment is the same, ϕ , for both weak and strong fields. We do not, however, presume any particular expression for the amplitude P_0 ; in fact, our consideration does not require such an expression.

Instead, it is enough for our conclusions that P_0 is a positive, monotonic, rapidly increasing function of \tilde{E}_1, \tilde{E}_2 . A physical ground for such an assumption is the fact that the intensity of high-order harmonics rapidly increases, on average, with the intensity of the pumping.

Using this model, we have shown that the optimal phase-matching conditions estimated within the perturbation-theory limits, would present a quite accurate approximation for nonperturbative HDM as well.

2.iii. Super-dressed two-level atom:

very high harmonic generation and multi-resonances [4,21,23,26,27,35,37,39-41,43,44]

Very high-order odd harmonic generation (HHG) by intense optical laser radiation in rare gasses and some ions discovered recently drastically deviates from the perturbation theory predictions by forming a so-called "plateau". The major features of HHG, in particular the plateau, result mainly from general properties of atomic nonlinear response. The direct numerical simulation of the *Schrödinger* equations for many-electron atoms using Hartree-Slater approximation requires tremendous amount of calculations and involves many processes, making it difficult to gain simple insights. Some simplified models, while reproducing some features of HHG, failed to generate simple results or to relate to experiments. We found that a two-level model [4,21,24,28,28] that not only reproduces experimentally observed plateau, but also allows us to evaluate its characteristics in explicit analytic form and predict new dramatic effects.

Rare gasses and rare-gas-like ions in which HHG has been observed so far, may not be inconsistent with two-level description as far as HHG is concerned. The energy E_1 of the first excited level of a rare-gas atom is fairly large ($R = E_1/\hbar\omega \gg 1$) and very close to the ionization limit E_{ion} , so that $\Delta E \equiv E_{ion} - E_1 \ll E_{ion}$, and $\Delta E \sim \hbar\omega$ where ω is the driving frequency. Thus, virtually *all* the higher harmonics may "see" a cluster of atomic levels between E_1 and E_{ion} as a *single* level (with effective parameters determined by all the contributing levels, with a strong dominance of the first excited level).

Starting from density-matrix equations for a two-level atom with relaxation, we generated typical plateau-like HHG spectra. We obtained also very simple analytic formulas which relate all characteristic of HHG to the energy of the first excited level, $E_1 = \hbar\omega_0$ (rather than to E_{ion} , which they are usually attributed to) and to the energy of interaction, $\hbar\Omega_R = \vec{d}\vec{E}$, where Ω_R is Rabi frequency, \vec{d} is a dipole moment, and \vec{E} is the driving field. These formulas are consistent with the available experimental data. In particular (i) the cutoff frequency of the plateau is determined as $\nu \equiv N_{cut}/R \approx (1 + 4\mu^2)^{1/2}$, which allows for comparison of different atoms driven by different lasers; here N_{cut} is cutoff harmonic number of the plateau, $R = \omega_0/\omega$, and $\mu \equiv \Omega_R/\omega$. Fig. 7a shows a theoretical straight line in the space of parameters ν^2 and $|E|^2 \propto \mu^2$, and available experimental points for Xe. (ii) The critical μ required for the plateau to appear at all, is evaluated for $R \gg 1$ as $\mu_{cr}^2 \approx 1/R$, or $(\Omega_R)_{cr}^2 \approx \omega_0 \omega$. Writing $\mu^2 = \beta \cdot I$, where I is the driving intensity in 10^{13} W/cm^2 and $\beta \approx 0.47$ is coefficient found by us from the plot in

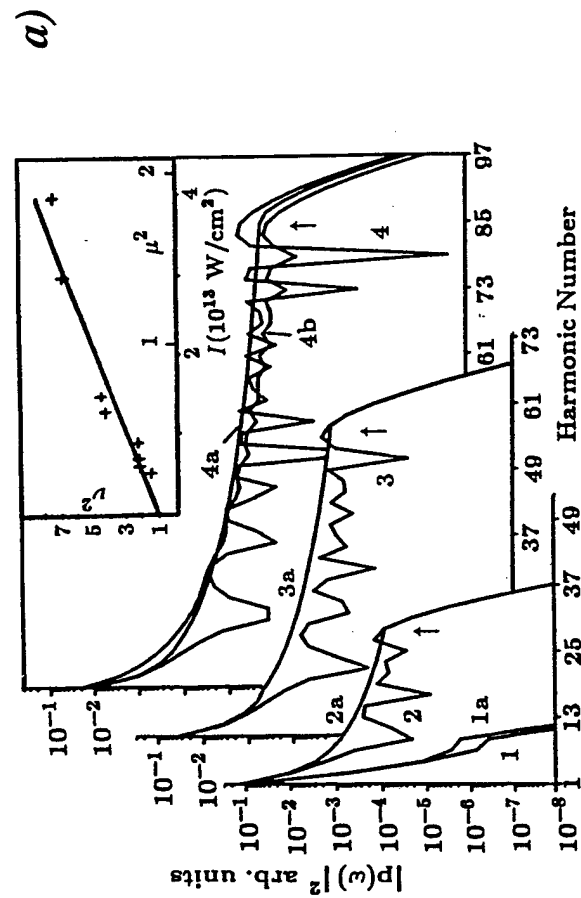
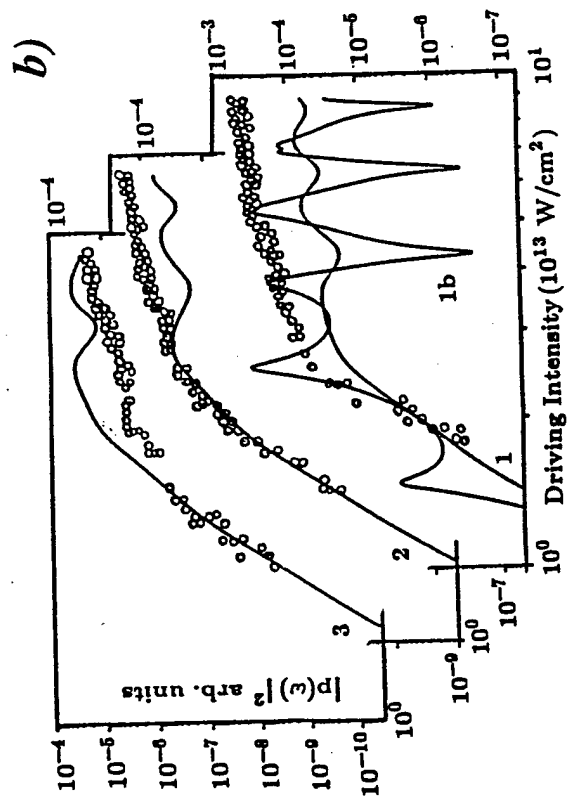


Fig. 7. a) HHG polarization spectra, $|p_n|^2$ ($N=2n-1$ is harmonic order), for various dimensionless driving intensities, μ^2 , and $R=7.24$ and $\Gamma=10^{-3}$ (except 4b where $\Gamma=0.1$). Curves: 1 -- $\mu=0.4$, 2 -- $\mu=2$, 3 -- $\mu=4$, 4 -- $\mu=6$; (1-4)a -- respective envelope approximations. Arrows indicate plateau cutoff points. Inset: Cutoff ratio square, v^2 , vs μ^2 for Xe. Crosses -- experiment [47,48], solid line -- linear fit.

b) p_n^2 vs μ^2 for $R=7.24$ (Xe + Nd:YAG laser) and various N . Solid lines -- theory ($\Gamma=0.1$, except 1b, where $\Gamma=0.01$), circles -- experiment [49]. Curves: 1 -- $N=17$, 2 -- $N=19$, 3 -- $N=21$.

c) Multi-resonances in population difference, x_0 , (a), and eigen-frequency λ_0 in the (0,1) domain, (b), vs amplitude μ , for $R=4.25$. Curves in (a): 1 -- $\Gamma=10^{-3}$; 2 -- $\Gamma=0.1$; 3 -- envelope approximation.



I is the driving intensity in 10^{13} W/cm^2 and $\beta \approx 0.47$ is coefficient found by us from the plot in Fig. 7a, we evaluate critical intensity for Xe as $5.5 \times 10^{12} \text{ W/cm}^2$ which compares well with the experiment, $5.0 \times 10^{12} \text{ W/cm}^2$. (iii) The onset of saturation (as μ increases) occurs at different intensities for each individual harmonic N : $\mu_{sat}(N) \approx N/2R$, or $(\Omega_R)_{sat} \approx N\omega/2$. Using again $\beta \approx 0.47$, we were able to closely fit, Fig. 7b, experimental and theoretical data on N -th harmonic intensity (for $N=17, 19, 21$) vs driving intensity (the theoretical curves 1-3 correspond to averaged polarization.) We found that similarly good fit could be attained for harmonics 15 through 9, by reducing $\beta^{1/2} \propto d$ by factor of 1.2 to 1.5. A significant feature of HHG found by us and consistent with other models is intensity-induced resonances in HHG (Fig. 7b, curve 1b for long driving pulses, linewidth $= 10^{-2}$.) Very pronounced and almost periodical with the amplitude μ are also multi-resonances in the population difference (Fig. 7c). Using the Floquet theory and numeric simulations, we found that all these resonances coincide with the extrema of intensity-induced "super-Rabi" frequencies of the "super-dressed" two-level atom. In the limit $\mu \gg 1$ the spacing between any two adjacent resonances is $\Delta\mu \approx \pi/2R$, or $\Delta(\Omega_R) \approx \pi\omega/2$. These resonances may be observed using time-resolved spectroscopy with longer driving pulses. Aside from a possible HHG mechanism in rare-gas atoms or ions by optical lasers, our results suggest that HHG may also be produced in other media and frequency domains, e. g. by microwave sources (e. g. gyrotrons) in electron gas or plasma in magnetic dc field, or by IR-lasers (e. g. CO and CO_2 lasers) in gasses or even semiconductors.

2.iv. Modulation-Induced Inhibition of Dynamics and High Order Frequency Mixing in a Periodically Driven Two-level Atomic System [13,53,56]

Electromagnetically induced transparency (EIT) of three-level atoms in a strong laser pulse is attracting a growing interest motivated by e. g. such applications as enhancement of nonlinear susceptibility and nonlinear frequency transformation. Its successful exploration provides stimulating background for the search for other field-induced transparency effects. We demonstrated the feasibility of a modulation-induced inhibition of dynamics (MID), self-transparency and very high order frequency mixing (HFM) in two-level system (TLS) subjected to a periodically modulated laser field. In contrast to self-induced transparency (SIT) in 2π solitons characterized by the dramatic dynamics of population, in MID the TLS dynamics (i. e. the oscillations of both the population and polarization) is almost fully suppressed. For a sinusoidal modulation, the conditions for MID coincide with those for the resonances occurring if the frequency of modulation, Ω_M , is close to a subharmonic of the averaged Rabi frequency, $\overline{\Omega_R}$. It has also been shown [4] that similar resonances in TLS may occur even when the system is driven by a cw (nonmodulated!) field strong enough to "super-dress" TLS by having Ω_R exceeded the TLS unperturbed frequency, ω_0 . We showed that at these resonances, in addition to the suppressed population difference, δ , the TLS *driven* polarization, p , vanishes too, resulting, together with vanishing δ , in the collapse of "Rabi sphere". Even as the spectral components of the driving field are strongly off the resonance, the field-induced Rabi-splitting

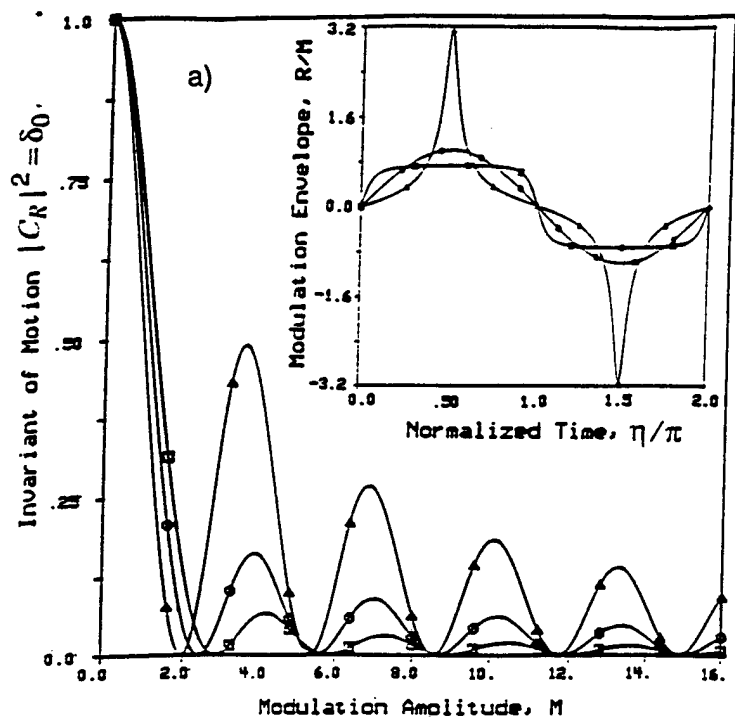
brings TLS at the MID points into exact resonance with the field. MID results in a self-transparency for the entire spectrum of the incident field (which could be very broad), allowing its propagation without dispersion suppressed now over the spectrum.

In a relaxationless TLS, if its dynamics is characterized "globally" by a Rabi sphere radius, C_R , with $C_R^2 = \delta^2 + p^2$, one finds that C_R is a (so called Casimir) invariant ($= 1$) independent of the driving field. However, in the modulation-driven TLS with *relaxation* (even when it is asymptotically *vanishing*), the radius C_R , although remaining constant in time, can be less than unity even *outside* of MID resonances (Fig. 8a). This inhibition is dominated by the population difference, $\bar{\delta}$, averaged over the modulation period. For the so called full modulation, we found that $C_R^2 = \bar{\delta} = \overline{\cos\Phi}$, where Φ is a Rabi phase. This result is valid for *any* periodic modulation.

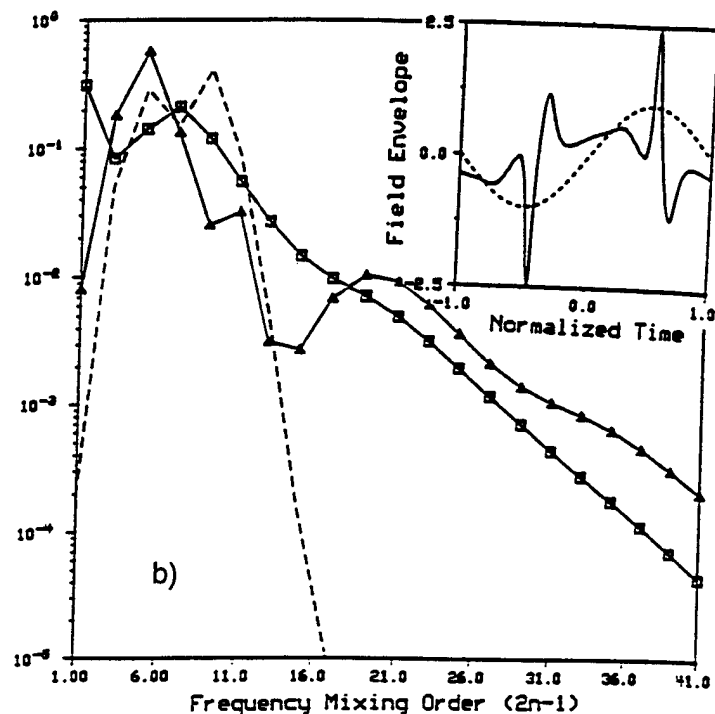
The MID resonances occur only at certain ratios $M = (\Omega_R)_{\max}/\Omega_M$ (usually around $M \approx \pi n$, where n is an integer). However, even more interesting effects occur *outside* of these resonances, where the periodic modulation induces dramatic TLS dynamics that can give rise to HFM. We found a parallel between HFM and recently discovered high harmonic generation (HHG) by very intense optical fields in rare gases, whereby, beginning at some harmonic order, the harmonics have the same order of amplitude up to some cutoff frequency, forming a spectral plateau followed by a rapid fall-off (see Fig. 8b). One of the simplest pertinent models of HHG is an overdriven TLS allowing an analytical solution [4] for the cutoff. We showed that a TLS-generated HFM spectrum, $\omega_n = \omega \pm (2n + 1) \Omega_M$, $n = 0, 1, 2, 3, \dots$, features a similar plateau, with a cutoff point, $\Omega_{\text{cut}}/\Omega_M \approx \sqrt{4 + M^2}$, similarly to [4]. Unlike HHG, during the propagation, HFM demonstrates large conversion efficiency, with the fundamental components almost vanishing at some points and their energy transversed into higher spectral components. This process gives rise to a train of soliton-like pulses, with the energy redistributed to produce short spikes of high peak intensity, with the individual length of each $\tau_M \approx \pi/(\Omega_M \sqrt{4 + M^2})$. (If $\lambda_0 = 1\mu\text{m}$, $\Omega_M/\omega_0 = 1.5\%$, and $M \approx 10$, $\tau_M \approx 100\text{ fs.}$) Our computer simulations (Fig. 8c) show the universal effect of the full revival of the field envelope and its spectrum after certain propagation distances determined by the boundary conditions. HFM can be used for coherent generation of new frequencies (e. g. for nonlinear spectroscopy) and of short pulses of high intensity. The MID and HFM effects can be observed in a configuration similar to SIT (using now a continuously modulated wave instead of a short pulse), or subharmonic resonance experiments (using now long propagation path and observing the field transformation).

2.v. Bright-bright 2π -Solitons in Stimulated Raman Scattering [6]

It is well known that the stimulated Raman scattering (SRS) may result in formation of peculiar solitons which combine a so called bright (regular) soliton at the pump (laser) frequency and a so called dark soliton (a deep minimum in the intensity profile), at the Stokes frequency. Following experimental observations, most of the theoretical work neglected the change of populations at the Raman quantum transition. If the population at the Raman



a) The invariant of motion, $C_R^2 = \delta_0^2$ (C_R - Rabi radius), vs the amplitude of modulation, M , for the modulation in the form of regular sinusoid (C), "flattened" sinusoid (\square), and "sharpened" sinusoid (Δ). The respective modulation envelopes are depicted in the insert.



b) The HFM spectra [spectral intensities normalized to their full sum, vs the HFM order: $2n-1$], of the polarization, p (dashed), at the boundary ($\zeta=0$), and of p (Δ) and the field envelope, R (\square) at $\zeta = 2348/Q$ (the total spatial cycle is $\zeta_c = 4950/Q$), when $M = 10.2$. Insert: R vs normalized time, τ/π , at $\zeta = 0$ (dashed) and at $\zeta = 2348/Q$ (solid).

c) The spatial dynamics of HFM: spectral intensities, $|R_{2n-1}|^2$ of the $(2n-1)$ -th harmonics of the envelope, R , vs the normalized propagation distance, ζ , for $M=3.5$.

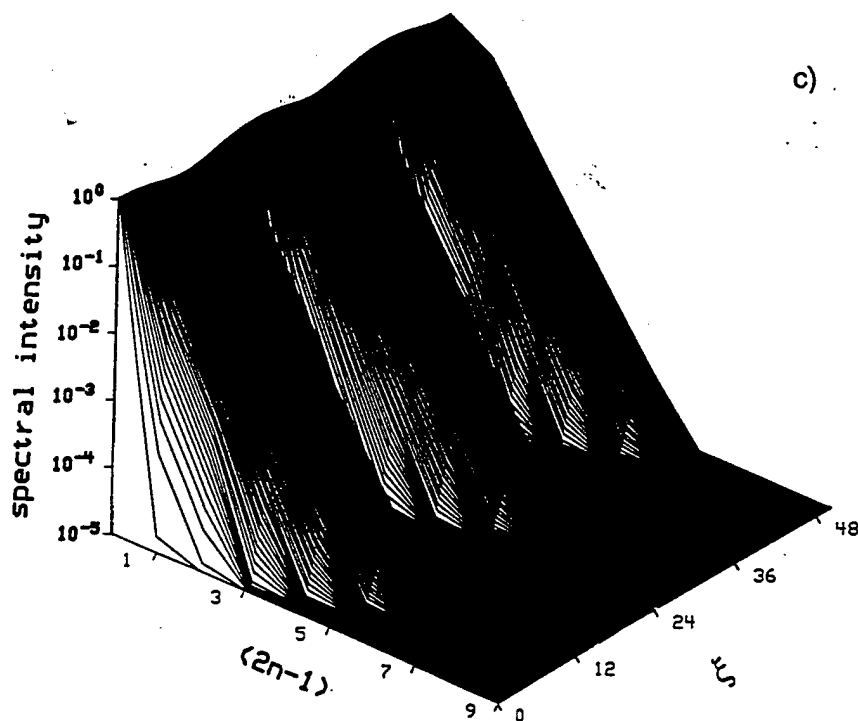


Fig. 8

transition is an essential part of the pulse dynamics (and if there is a nonvanishing dispersion), it may result in 2π -pulses to the extent similar to self-induced-transparency solitons, consisting in the case of only two components, of bright solitons at the pump and Stokes components, both having a surprisingly simple, Lorentzian envelope. Theoretically discovered a long while ago, these solitons have not been observed experimentally, which may be attributed to their threshold nature which imposes some limitations on the pulse frequency and length for the most of the materials traditionally used for SRS. We have proposed [6] conditions for experimental excitation of these solitons and develop the theory for the case of three components (e. g. laser+Stokes+anti-Stokes or laser+Stokes+2nd Stokes) [63] which may broaden possibilities of exploration of new solitons.

The major characteristic of the bright-bright SRS soliton is that it is a "threshold" soliton: its parameters (the duration, τ , photon flux, Φ , and the total number of photons, P_{Σ} , must satisfy threshold conditions, $\tau < \tau_{cr}$, $\Phi_0 > \Phi_{cr}$, and $P_{\Sigma} > P_{cr}$, where the respective threshold (critical) values for the two-component soliton are: $\tau_{cr} = \delta_{SL}/|w_{SL}|$; $\Phi_{cr} = 4\pi N_a/\delta_{SL}$; and $P_{cr} = 2\pi N_a/|w_{SL}|$; here, δ_{SL} and w_{SL} are related to the media dispersion and Raman polarizabilities. These conditions, which impose some limitations on the parameters of both a medium and a driving field, in particular, on the soliton duration has never, to the best of our knowledge, been addressed in the literature. Our estimates show that for the most of the typical SRS media, τ_{cr} may be as short as a few femtoseconds, which might be one of the reasons the bright-bright soliton has not been observed yet. Thus the major requirement is the selection of material and laser frequency. A natural choice is electronic SRS in alkali metal vapors, e. g., Cs vapor, with its high (up to 50%) conversion efficiency. For the lasers $\lambda_L = 420 - 530 \text{ nm}$, one can show that resonant enhancement is necessary for the feasibility of the bright-bright solitons. Such enhancement might be provided by tuning the pumping laser in such a way that the Stokes radiation is resonant to a Cs $6p-5d$ transition, and using another laser to slightly populate $6p$ level. Our estimates show that all the threshold conditions would be fulfilled if an additional, 852.34 nm , laser populated Cs $6p_{3/2}$ level; this would also provide the control of the soliton. Another interesting opportunity could be presented by optical fibers, where, due to larger dispersion, the limitations on the soliton length could be relaxed.

2.vi. Non-oscillating high-intensity subfemtosecond solitons [9,14,17,19,49,50,52,54,55,57,60]

We proposed, and began pilot research on, two ways of generating high-intensity subfemtosecond (down to $\sim 10^{-16} \text{ s}$) pulses and solitons of very high intensity (up to $\sim 10^{16} \text{ W/cm}^2$) and very high repetition rate. This newly originated research was planned by us to be continued on full-scale under our new AFOSR grant; our current research is proceeding according these plans.

Within the last 10 years, the physics and technology of EM-radiation witnessed a few fascinating discoveries, inventions, and developments that bear a promise for a tremendous

expansion of the field in the near future. The barriers that seemed unsurmountable until very recently, have been broken following pioneering work of several research groups. We believe that the time has come to push the envelope in yet another direction. Our newly initiated research is focused on the possible physical phenomena in nonlinear optics, which would allow one to generate super-short EM pulses, with duration from 10 fs down to 0.1 fs, or 100 attosecond, of very high intensity up to $10^{14} - 10^{16} \text{ W/cm}^2$, and with no carrier oscillations (unipolar, or nonoscillatory, pulses). Each individual pulse of such a nature, ideally, is just a singular burst of EM field, which can be described as a "half-cycle" pulse. The soliton form of such a pulse is called by us an "Electromagnetic bubble" (EMB). An EMB would have a continuous power spectrum ranging from zero frequency to the highest (cutoff) frequency of the pulse, $\omega_{cut} \sim 2.6/\tau$, where τ is the pulse duration (evaluated at the half-intensity), such that e. g. for $\tau = 0.2 \text{ fs}$, the cutoff wavelength, $\lambda_{cut} = 2\pi c/\omega_{cut} \sim 2.4 c \tau$, is $\lambda_{cut} \sim 1440 \text{ \AA}$, i. e. in the far ultra-violet. It would be seen by a human eye as an extremely short and powerful *burst of white light*, to a great extent similar to that originated by an *atomic explosion*. Even a 1 fs long pulse will have a cutoff wavelength $\sim 7200 \text{ \AA}$, with its spectrum still covering the entire *infrared, millimeter, microwave, and rf* domains.

These super-short and intense unipolar pulses might be of great interest for the host of applications. They can be used for a "global" spectroscopic technique based on a shock-like excitation across the entire atomic spectrum (to the extent similar to passing atoms through a foil), including the normally prohibited transitions. The ionization by a pulse shorter than the orbital period may bridge a gap between conventional photoionization and collisional ionization by a particle; it can also provide an exciting opportunity to pick up an electron at a certain point of its orbit, provided its phase has been prepared before the event. Time-domain spectroscopy of dielectrics and semiconductors with these pulses may expand this method from presently available THz domain to optical frequencies. The need in such pulses is obvious in time-resolved spectroscopy of transient chemical processes occurring on a femtosecond time scale, e. g. dissociation and autoionization, and especially for quantum control of chemical transformations. The train of subfemtosecond pulses with very high repetition rate ($\sim 100 \text{ THz}$, or with the spacing $\sim 10 \text{ fs}$), which, as proposed here, can be obtained using cascade stimulated Raman scattering, can be used for very high speed stroboscopy by making series of snap-shot atomic motion in a molecule (e. g. during its dissociation), similar to stroboscopic images of a flying bullet.

Applications of EMB can be envisioned for the defense technologies. They can be used for the super-broad bandwidth EM-jamming system, and as a radiation source rendering blind infrared night-vision devices on the ground, or infrared homing devices of heat-seeking anti-aircraft missiles and rockets.

Different materials will have different transparency for new pulses, which can facilitate a great number of possible applications, based on the use of EMBs, emulating the functions of X-rays. They can be used for monitoring processing of high-density computer chips, for

screening food products at the food-processing facilities, luggage in the airports, concealed (even nonmetallic, using contrast between plastic and human tissues) weapons, etc.

**2.vi.1. Subfemtosecond pulses in mode-locked 2π -solitons of
the cascade stimulated Raman scattering [9,17,19,49,50,52,54,55,60]**

One approach of attaining sub-fs pulses is based on multi-frequency cascade Raman stimulated scattering (CSRS). We predicted that pump laser wave with the frequency ω_L and many cascade-excited Stokes and anti-Stokes component with their frequencies $\omega_j = \omega_L + j\omega_0$, $j = \pm 1, \pm 2, \pm 3...$, can be mode-locked to each other through a fast "full-swing" 2π -nutations of population at the Raman transition with the frequency $\omega_0 \ll \omega_L$. Similarly to "bright-bright" 2π -solitons in CSRS with two and three [6] components, these solitons have a new, very simple, Lorentzian intensity profile. Due to the engagement of many mode-locked components, however, their total EM field in the time domain consists of the train of ultra-short, of the order of the pump cycle, $2\pi/\omega_L$, or even *shorter*, pulses separated by the interval $2\pi/\omega_0$. The major feature of the proposed effect is that *all* the frequency components of the new soliton are so called bright solitons, in contrast to the well known bright+dark soliton combination in SRS. The high-order CSRS required to observe the proposed effect has been observed experimentally in many experiments, with the total number of components up to ~10-15.

In order to attain SFP generation, the main problem to be solved is to "lineup" the multiple CSRS components, i. e. to phase-lock them and force them to propagate with the same group velocity to overcome walk-off effect. The super-short pulses considered here are the result of coherent interference of all the participating CSRS components, which have to be present in the same space/time area over sufficiently long interaction path. Without a "component-locking", the walk-off effect might disallow the pulse formation, since the group velocities of different CSRS components over such a large spectral stretch can be substantially different. We predicted that in general case of multi-CSRS [9], as well as for simpler 2- and 3-component SRS [6], this problem can be solved by formation of multi-component solitons, whereby all the Raman components are mode-locked within a 2π soliton reminiscent of the self-induced transparency (SIT) solitons and related to the quantum dynamics at the Raman transition. One of the results of the mode-locking is that all of these soliton components propagate with the same group velocity (although their linear group velocities are different), have the same amplitude shape, and fully overlap in time and space. The coherent interference of *many* (instead of two or three) participating mode-locked frequency components gives rise to the train of SFPs (spaced by $2\pi/\omega_0$) with their length being $\sim 2\pi/\omega_{mx}$ (where ω_{mx} is the highest anti-Stokes component frequency), i. e. much *shorter* than the pump cycle, $2\pi/\omega_L$. This effect, in which the 2π -soliton plays a role of traveling shatter, can, to the extent, be related to mode-locked laser pulses formed by the coherent interference of many modes.

2.vi.2. "Electromagnetic Bubbles" [14,17,60]

Another process capable of producing very short, potentially subfemtosecond pulses, is the soliton formation in gases. We showed that atomic gases can support solitary pulses of a unipolar, nonoscillating electromagnetic field ("EM-bubbles") with the amplitude of up to the atomic field ($\sim 10^9$ V/cm), with their length from $\sim 10^{-9}$ s to $\sim 10^{-16}$ s. EM-bubbles propagate without dispersion and are insensitive to the change of gas density. Using computer simulation, we showed that EM bubbles can be formed out of unipolar pulses that are already available experimentally (or are within the reach of existing techniques), propagating in dense Xe. Atomic gasses can also support an EM shock wave forming a precursor of a cw ionizing field.

To demonstrate the main idea, we considered general Maxwell + Bloch (or classical constitutive) equations for this problem, and discussed their general stationary (solitary) wave solution, in particular, solitons -- EM-bubbles. We showed that these pulses may propagate without dispersion and are stable and insensitive to the change of gas density. We showed that atomic gasses can also support an EM shock wave which is a precursor of a cw ionizing field. We proposed a few directions of research to further explore these solitons and their possible applications.

All the experimentally observed time-domain solitons in nonlinear optics are so called envelope solitons, i. e. quasi-harmonic oscillations modulated by an envelope much longer than a single cycle of the carrier wave, with their spectral width substantially smaller than their carrier frequency. Many applications, however, in particular the study of atomic physics by means of photoionization, call for short and intense EM-pulses of *nonoscillating* nature, with their spectrum spread from zero to some cutoff frequency. Especially significant are nonoscillating *solitary* waves able to propagate over substantial distances with unchanged shape and length.

We showed that such solitons are not only feasible (and some of them -- with much lower incident intensities), but also a natural process for many nonlinear system, both quantum and classical. Their length may range from a small fraction of the cycle length of the resonance that supports them, to much longer than that cycle, depending on their intensity. We call them EM-bubbles (EMB) to stress their non-envelope nature. We showed that with the light intensities available now, these EMBs can be as short as 10^{-16} s. We demonstrated that the photoionization imposes an upper limit on the EMB amplitude and a lower limit on its length; after an EMB reaches its shortest length at some peak amplitude, the further increase of the amplitude results in EMB broadening. At some threshold amplitude, the EMB degenerates into a shock wave of ionization.

2.vii. Two-photon induced fluorescence of biological markers using optical fibers [15]

Stimulated by our interaction and collaboration with the Johns Hopkins University School of Medicine, we began a bio-nonlinear optics research, choosing multiphoton processes as a promising direction. The use of fluorescent dyes which can be attached to specific cellular components, as biological markers, has become a well-established biomedical technique in recent years. When optically stimulated, these dyes emit a characteristic fluorescence, enabling the structure and organization of the sample to be studied and visualized by means of fluorescence spectroscopy and confocal microscopy. Typical dyes used in biological studies absorb and emit visible or UV light. UV light, however, is strongly absorbed within a thin layer near the surface of the sample. This, and other problems with UV pumping, including the lack of inexpensive UV laser sources, photobleaching of the dye molecules, and the anticipated photodamage of living cells, be overcome a technique that employs two-photon absorption in the dye, two-photon induced fluorescence (TPIF). TPIF, however, encounters its own problems, the most obvious being its apparent inability to probe the inhomogeneous media widely present in biological research. Such media severely scatter incident laser light, thus preventing the tight focusing needed to observe TPIF, and seemingly limiting TPIF applications to investigating layers near the surface. We believe that this shortcoming can be compensated for by using optical fibers to deliver the pump light into the inhomogeneous medium and to extract the TPIF signal. We have done preliminary experiments [15] on TPIF with fibers delivering pump radiation into some dye solutions. Our first experimental results have shown feasibility of the effect. We plan to continue with the experiments.

2.viii. Other research

2.viii.1. Eigenmodes of $\chi^{(2)}$ wave-mixings: cross-induced 2-nd order nonlinear refraction [1]

Second-order nonlinear interactions are some of the most basic, best known and widely used processes in nonlinear optics. They can be viewed as a three-wave mixing, whereby waves at only three interacting frequencies ($\omega_1 + \omega_2 = \omega_3$) are phase-matched. In general case, these interactions presume energy exchange between all of three waves. It is known also that there are special regimes of three-wave mixing (which could be regarded nonlinear eigenmodes) whereby there is no energy exchange between any of those three waves; these no-interaction-modes are usually of no interest to frequency transformation or amplification applications. We show [1], however, that the interaction between the three waves in these eigenmodes is still manifested by linear (with respect to the distance of propagation) phase change in each of the waves as they propagate. For these $\chi^{(2)}$ eigenmodes to occur, a certain relationship should be pre-arranged between all three intensities (as well as phases) of the waves. Peculiar phase property of these eigenmodes is essentially equivalent to the amplitude-dependent and phase-sensitive change of phase velocity of each of the waves (with

their intensities unchanged) as they propagate. This property makes the $\chi^{(2)}$ eigenmodes ideal candidates for $\chi^{(2)}$ cross-induced nonlinear refraction, i. e. amplitude-dependent phase velocity, emulating the third-order nonlinear refractive index, in particular, in the "cascade" second-harmonic generation (SHG). The eigenmodes constitute the only 2-nd order nonlinear process with the unchanging amplitude, and with the phase changing *linearly* with the distance of propagation, and thus are the only true example of " $\chi^{(2)}$ nonlinear refraction".

Compared to the modes in which only SHG was utilized, the eigenmodes offer broader opportunities involving in general case *three* waves with more independently controllable parameters. Using the well known coupled equations for the spatial dynamics of the waves in three-wave mixing, we found that the condition on the intensities $I_j \equiv I(\omega_j)$ of all three field for the eigenmode to exist, is $\pm \alpha \sqrt{I_1 I_2 I_3} (\omega_1/I_1 + \omega_2/I_2 - \omega_3/I_3) + c \Delta k = 0$ where $\alpha \propto \chi^{(2)}$ is coefficient of nonlinearity, and Δk is the phase mismatch. In such a case, the rate of spatial change of phases at each frequency ω_j , i. e. "nonlinear refraction" at ω_j , is $\beta_j = \mp \alpha k_{0j} \sqrt{I_1 I_2 I_3} / I_j$, $j = 1, 2, 3$ and k_{0j} are respective vacuum wave numbers for each frequency. To maintain the eigenmode, the "combined" phase Φ of the interaction must be equal to 0 or π . >From the nonlinear refraction point of view, the $\chi^{(2)}$ eigenmodes have a very peculiar property distinguishing them from $\chi^{(3)}$ nonlinear refractivity: the nonlinear changes of phase velocity (i. e. β_j), can be either positive or negative for the *same* intensities of all of the three waves, depending of the phase, Φ , at the boundary of incidence. Our calculations also showed that all these eigenmodes are spatially stable. Thus, cross-induced 2-nd order nonlinear refraction can be used for amplitude-phase and phase-phase nonlinear control in $\chi^{(2)}$ materials combining advantages of relatively large $\chi^{(2)}$ nonlinearity with emulated nonlinear refractivity of $\chi^{(3)}$ materials.

2.viii.2. X-ray narrow-line transition radiation source based on low-energy electron beams traversing a multilayer nanostructure [16]

Some time ago, this PI suggested that soft-X-ray resonant transition radiation can be generated by relatively low-energy electrons if they traverse a periodic multilayered solid-state structures (nanostructures) with layers thinner than $\sim 50\text{--}100\text{ nm}$. In this research, he has returned to the subject [16], in view of recent developments in the fabrication of nanostructures, electron beam techniques, and new opportunities for applications.

In the previous work, resonant TR was treated without taking photoabsorption and electron scattering into consideration. In solids, however, too slow electrons ($E_0 < 50\text{--}100\text{ keV}$) may be ineffective because of electron scattering. Now we show [18] that, fortunately, a moderate increase in the electron energy above this level will render the loss of electrons insignificant. After taking both photoabsorption and electron scattering into consideration, we obtain the optimal range of electron energy ($10^5 \text{ -- } 10^6\text{ eV}$ for soft X-rays with photon energy of $\hbar\omega \sim 0.1 - 1\text{ keV}$), the optimal total thickness of the structure, and maximal radiation for each

given frequency ω , Tables 1 and 2.

Radiator	λ (Å)	l_{opt} (Å)	L_{opt} (μm)	η_{TR}	η_{BR}
Ba	16.90 (0.780 keV)	1329	13.8	3.37×10^{-6}	4.75×10^{-9}
Ce	14.04 (0.883 keV)	1269	7.2	1.80×10^{-6}	4.17×10^{-9}
Eu	11.00 (1.127 keV)	979	11.3	7.72×10^{-7}	4.50×10^{-9}
Ge	10.19 (1.217 keV)	988	10.2	1.33×10^{-6}	2.24×10^{-9}

Table I. The optimal spatial period l_{opt} , radiation efficiency of TR η_{TR} and of Bremsstrahlung η_{BR} , and optimal total length L_{opt} for nanostructures made of Be/Ge, Be/Ce, Be/Ba, or Be/Eu at the TR peaks related to an absorption edge of the heavier element in each combination (the L edge for Ge, and M edges - for the Ba, Ce, and Eu). $E_0 = 4.5$ MeV, the emission angle $\theta_1 = 0.573^\circ$.

Radiator	λ (Å)	l_{opt} (Å)	L_{opt} (μm)	η_{TR}	η_{BR}
Ba	16.90 (0.780 keV)	1396	9.07	2.21×10^{-6}	3.19×10^{-9}
Ce	14.04 (0.883 keV)	1297	5.97	1.57×10^{-6}	3.55×10^{-9}
Eu	11.00 (1.127 keV)	982	9.48	7.17×10^{-7}	3.90×10^{-9}
Ge	10.19 (1.217 keV)	993	9.01	1.26×10^{-6}	2.09×10^{-9}

Table II. The same as in Table I except that in each material couple Be is replaced with C.

One of the major new factors considered by us here in applications to TR in solid-state nanostructures, is the proposed use of very narrow spectral resonances of the dielectric constant of the atomic inner-shell (in particular, K, L, and M-shells) absorption edges of the constituent materials. It is well known that due to photoionization of bound electrons, the absorption spectra of atoms in the X-ray domain show almost discontinuous jumps at the so called absorption edges. This phenomenon is widely used in the experimental research and spectroscopic and radiation sources technology. However, a related phenomenon of strong resonances of a real component of dielectric constant, ϵ , at the absorption edges, has never, to the best of our knowledge, been used in application to radiation sources. The resonant dispersion can result in ϵ significantly exceeding 1 at a resonance (in contrast to its regular plasma-like behavior in the X-ray domain, whereby $\epsilon(\omega) < 1$). This strongly resonant anomalous dispersion of $\epsilon(\omega)$ results in drastic changes of $[\epsilon(\omega)_1 - \epsilon(\omega)_2]^2$ with the wavelength at the absorption edges of both the materials, and thus facilitates the formation of strong TR lines at these resonances. An absorption edge itself is instrumental in further narrowing of TR lines, Figs. 9 and 10.

To explore prospects for practical applications of resonant TR, we briefly compared its spectral brightness with that of the sources already in use. We have shown that transition

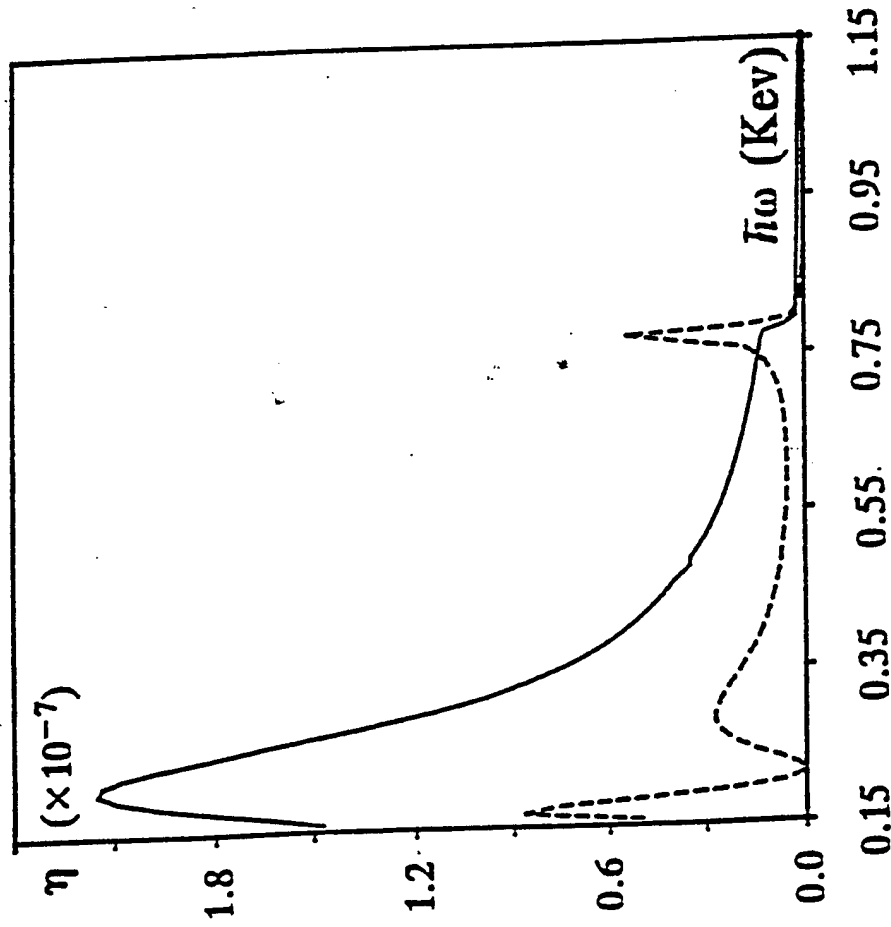


Fig. 9 Normalized TR efficiency η in number of photons per electron per 1 eV photon energy per 1 MeV electron energy vs photon energy $\hbar\omega$ in keV: Be/Ba nanostructure, $E_0 = 1$ MeV. The curve in solid line is calculated with plasma frequency formula, Eq. (28), while the curve in dashed line is calculated with the atomic scattering factors, Eq. (35).

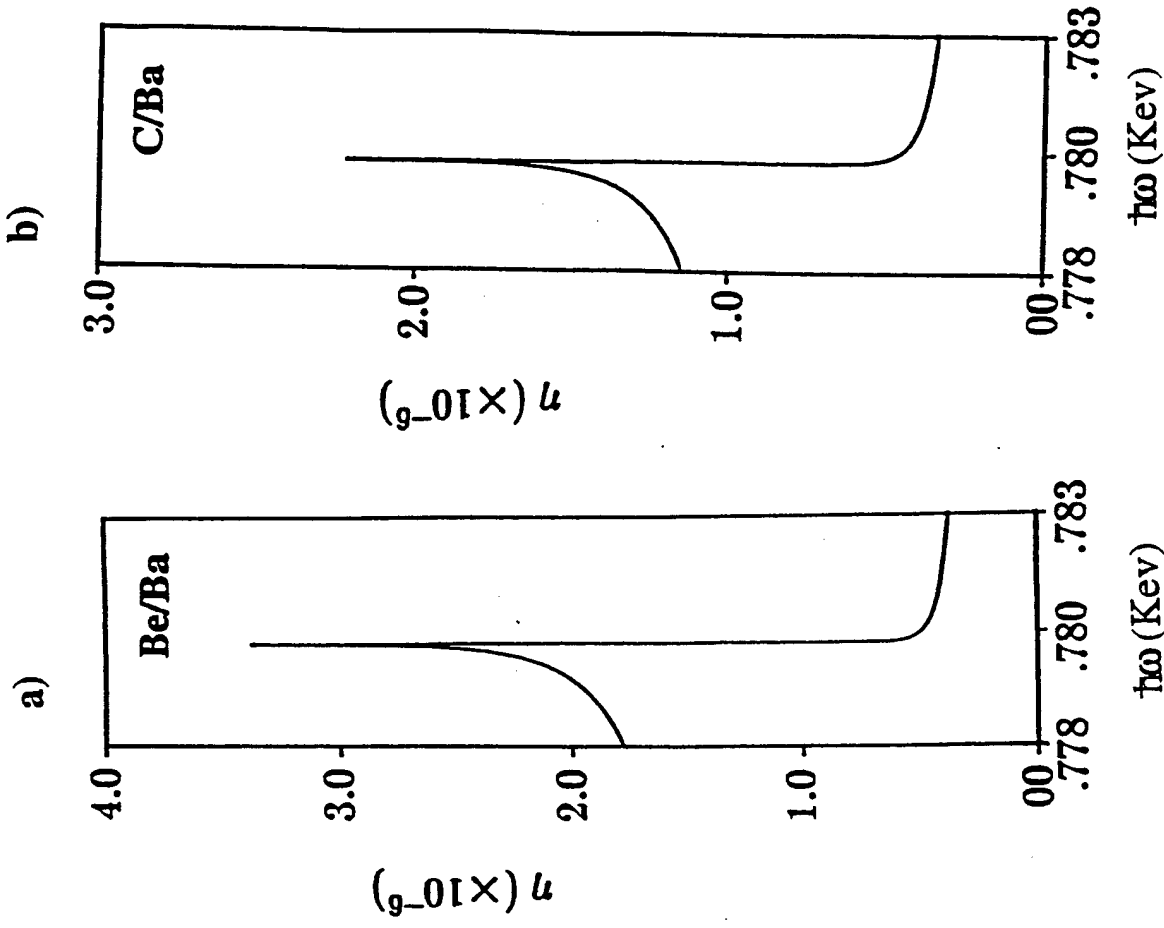


Fig. 10 Normalized radiation efficiency $\eta = \eta_{TR} + \eta_{BR}$, with Bremsstrahlung radiation included, in number of photons per electron per 1 eV photon energy per 1 MeV electron energy vs photon energy $\hbar\omega$ in keV, for the nanostructures made of a) Be/Ba, and b) Be/C. $E_0 = 4.5$ MeV, and the spatial period L and total length L are optimized at the Ba absorption edge.

radiation sources using multilayer TR radiators optimized at absorption edges and based on commercially available small-scale electron accelerators could be among the brightest laboratory (non-synchrotron) X-ray sources, and compete with LPP in applications, e. g. scanning X-ray microscopy.

A promising application of multilayer TR generators could be expected in computed tomography (CT). CT using synchrotron radiation demonstrates a number of advantages of synchrotron radiation over commonly used X-ray tubes. In particular, by taking two images at the two energies bracketing the K-edge of iodine (33.17 keV), one can achieve very high contrast; this is called multiple-energy CT (MECT). Energy spread (linewidth) of the imaging X-ray beam should be sufficiently small, preferably $\sim 0.1\%$. An experimental MECT system employs the photon flux of $\sim 2 \times 10^8$ *ph/s* with E_{ph} near the iodine K-edge. Although all the particular examples of radiating structures given so far have been optimized to radiate at photon energy near 1 keV, the TR photon energy of tens of keV is well within the scope of our consideration. Our preliminary calculations indicates that one may expect the photon flux of the same order of magnitude from resonant TR source, and, therefore, that TR radiation based on a solid-state nanostructure sources for MECT systems can be potentially competitive with synchrotron radiation while being possibly much more affordable for a large hospital or university.

3. Work published under AFOSR Grant F49620-93-1-0220

3.i Regular Journal Papers

- [1] A. E. Kaplan, "Eigenmodes of $\chi^{(2)}$ wave-mixings: cross-induced 2-nd order nonlinear refraction", Opt. Letts. 18: 1223-1225 (Aug. 1, 1993).
- [2] P. L. Shkolnikov, A. E. Kaplan, and A. Lago, "Phase matching for large-scale frequency upconversion in plasma", Opt. Letts, 18: 1700-1702 (Oct. 15, 1993).
- [3] A. E. Kaplan and G. A. Swartzlander, "Self-bending of light: comment", Opt. Letts. 19: 71 (Jan. 1, 1994).
- [4] A. E. Kaplan and P. L. Shkolnikov, "Super-dressed two-level atom: very high order harmonic generation and multi-resonances", Phys. Rev. A. 49, 1275-1280 (Feb., 1994).
- [5] E. Hudis, P. L. Shkolnikov, and A. E. Kaplan, "X-ray stimulated electronic Raman scattering in Li and He", Appl. Phys. Lett. 64, 818-820 (Febr. 14, 1994).
- [6] A. E. Kaplan, P. L. Shkolnikov, and B. A. Akanaev, "Bright-bright 2π -Solitons in Stimulated Raman Scattering", Optics Letters 19, 445-447 (Apr. 1, 1994).
- [7] E. Hudis and A. E. Kaplan, "Ionization-front Soliton in the X-ray Stimulated Raman Scattering" Optics Letters 19, 616-618 (May 1, 1994)
- [8] E. Hudis, P. L. Shkolnikov, and A. E. Kaplan, "X-ray stimulated electronic Raman scattering in neutral gases and inhibited ionization", JOSA B 11, 1158-1165, (July 1994).
- [9] A. E. Kaplan, "Subfemtosecond Pulses in Mode-locked 2π -Solitons of the Cascade Stimulated Raman Scattering", Phys. Rev. Lett. 73: 1243-1246 (29 August 1994).
- [10] P. L. Shkolnikov, A. E. Kaplan, and A. Lago, "Phase-matching optima for high-order multiwave mixing and harmonic generation beyond perturbation limit", Optics Communications 111: 93-98 (15 Sept. 1994).
- [11] P. L. Shkolnikov, A. Lago, and A. E. Kaplan, "Optimal quasi-phase-matching for high-order harmonic generation in gases and plasma", Phys. Rev. A 50: 4461-4464 (Dec. 1994).
- [12] A. E. Kaplan and E. Hudis, "Modulation-Induced Multi-Transparency, Inhibition of Dynamics and High Order Frequency Mixing in a Periodically Driven Two-level Atomic System", Laser Physics, 5: 479-485 (May-June 1995).
- [13] F. A. Weihe, S. K. Dutta, G. Korn, D. Du, P. H. Bucksbaum, and P. L. Shkolnikov, "Polarization of high intensity high harmonic generation", Phys. Rev. A, *Rapid Communications*, 51, R3433-6 (May 1995).
- [14] A. E. Kaplan and P. L. Shkolnikov, "Electromagnetic "Bubbles" and Shock Waves: Unipolar, Nonoscillating EM-Solitons", Phys. Rev. Lett. 75: 2316-2319 (18 Sept. 1995).
- [15] A. Lago, A. T. Obeidat, A. E. Kaplan, J. B. Khurgin, P. L. Shkolnikov, and M. D. Stern, "Two-photon induced fluorescence of biological markers using optical fibers", 20:

2054-2057 (15 Oct. 1995).

- [16] A. E. Kaplan, C. T. Law, and P. L. Shkolnikov, "X-ray Narrow-line Transition Radiation Source Based on Low-Energy Electron Beams Traversing a Multilayer Nanostructure", *Phys. Rev. E.*, 52: 6795-6808 (Dec. 1995).
- [17] A. E. Kaplan and P. L. Shkolnikov, "Subfemtosecond High-Intensity Unipolar Electromagnetic Solitons and Shock Waves", *Int. J. of Nonlinear Optical Physics & Materials*, 4: 831-842 (Oct. 1995).
- [18] P. L. Shkolnikov, A. E. Kaplan, and A. Lago, "Phase-matching optimization of large-scale nonlinear frequency upconversion in neutral and ionized gases", *JOSA B* 13: 347-354 (Feb. 1996).
- [19] A. E. Kaplan and P. L. Shkolnikov, "Subfemtosecond Pulses in the Multi-Cascade Stimulated Raman Scattering", *JOSA B* 13: 412-423 (Feb. 1996).

3.ii. Books and Book Chapters

- [20] A. E. Kaplan and P. L. Shkolnikov, "Prospects for X-ray nonlinear optics", in *Nonlinear Optics and Optical Physics*, I. C. Khoo, J. F. Lam, and F. Simoni, eds., World Scientific, 1994, v 2., p. 156.
- [21] A. E. Kaplan and P. L. Shkolnikov, "Super-dressed two-level atom: very high harmonic generation and multiresonances", in *Multiphoton Processes*, D. K. Evans and S. L. Chin, eds, World Scientific, 1994, p. 257.

3.iii. Conference Proceedings

- [22] P. L. Shkolnikov and A. E. Kaplan, "Resonant frequency transformations of short-wavelength coherent radiation in plasma", *OSA Proc. of Short Wavelength V: Physics with Intense Laser Pulses*, Eds. P. B. Corkum and M. D. Perry (OSA, Washington, DC, 1993), v. 17, pp. 239-242.
- [23] A. E. Kaplan and P. L. Shkolnikov, "Super-dressed two-level atom: very high order harmonic generation and multi-resonances", *OSA Proc. of Short Wavelength V: Physics with Intense Laser Pulses*, Eds. P. B. Corkum and M. D. Perry (OSA, Washington, DC, 1993), v. 17, pp. 156-158.
- [24] P. L. Shkolnikov, A. E. Kaplan, and A. Lago, "Phase matching for large-scale nonlinear frequency upconversion in plasma", *OSA Proceedings of Short Wavelength V: Physics with Intense Laser Pulses*, Eds. P. B. Corkum and M. D. Perry (OSA, Washington, DC, 1993), v. 17, pp. 137-140.
- [25] E. Hudis, P. L. Shkolnikov, and A. E. Kaplan, "X-ray stimulated electronic Raman scattering in non-ionized gases", *OSA Proc. of Short Wavelength V: Physics with Intense Laser*

- Pulses, Eds. P. B. Corkum and M. D. Perry (OSA, Washington, DC, 1993), v. 17, pp. 235-238.
- [26] A. E. Kaplan and P. L. Shkolnikov, "Super-dressed two-level atom: very high order harmonic generation and related phenomena" (*invited*), Proceedings of LEOS'93 (November 15-19, 1993, San Jose, CA), pp. 311-312.
 - [27] A. E. Kaplan and P. L. Shkolnikov, "Super-dressed two-level atom: very high harmonic generation and multi-resonances", Proceedings of Int. Conference on Multiphoton Processes (ICOMP VI), (1993, Quebec-City, Canada); Eds. D. K. Evans and S. L. Chin, World Scientific, Singapore, 1994, pp. 257-260.
 - [28] P. L. Shkolnikov, A. E. Kaplan, and A. Lago, "Phase-matching optima for high-order multiwave mixing beyond perturbation limit", in *Ultrafast Phenomena IX*, Eds. P. F. Barbara, W. H. Knox, G. A. Mourou, and A. H. Zewail (Springer-Verlag, New York, 1994-95), p. 263-264.
 - [29] M. Key and P. L. Shkolnikov, "Feasibility study of non-linear difference frequency generation in a laser produced plasma with a Ge XXIII XUV laser and a Nd glass laser", in *Rutherford Appleton Laboratory Report RAL-93-031*, 1993, p.84.
 - [30] P. L. Shkolnikov and A. E. Kaplan "X-ray + optical nonlinear mixing in plasma", in *X-ray Lasers 1994*, Eds. D. C. Eder and D. L. Matthews (AIP, New York, 1994-95), p. 478-482.
 - [31] P. L. Shkolnikov and A. E. Kaplan "X-ray nonlinear optics with high-order harmonics", in *X-ray Lasers 1994*, Eds. D. C. Eder and D. L. Matthews (AIP, New York, 1994-95), p. 522-524.

3.iv. Conference Papers

- [32] P. L. Shkolnikov and A. E. Kaplan, "Resonant frequency transformations of short-wavelength coherent radiation in plasma", Short Wavelength V: Physics with Intense Laser Pulses, March 29-31, 1993, San Diego, CA.
- [33] P. L. Shkolnikov, A. E. Kaplan, and A. Lago, "Phase matching for large-scale frequency upconversion in plasma", Short Wavelength V: Physics with Intense Laser Pulses, March 29-31, 1993, San Diego, CA.
- [34] A. E. Kaplan and P. L. Shkolnikov, "Plateau-cutoff formula for high harmonic generation in two-level atoms", Short Wavelength V: Physics with Intense Laser Pulses, March 29-31, 1993, San Diego, CA.
- [35] A. E. Kaplan and P. L. Shkolnikov, "Superdriven two-level atom: Analytic theory of very high harmonic generation and "super-resonances", Short Wavelength V: Physics with Intense Laser Pulses, March 29-31, 1993, San Diego, CA.
- [36] E. Hudis, P. L. Shkolnikov, and A. E. Kaplan, "X-ray stimulated electronic Raman scattering in non-ionized gases", Short Wavelength V: Physics with Intense Laser Pulses, March

29-31, 1993, San Diego, CA.

- [37] A. E. Kaplan and P. L. Shkolnikov, "Analytic plateau-cutoff formula for high harmonic generation in two-level atoms", QELS'93, May 2-7, 1993, Baltimore, MD.
- [38] A. E. Kaplan, "Eigenmodes of $\chi^{(2)}$ wave-mixings: cross-induced 2-nd order nonlinear refraction", QELS'93, May 2-7, 1993, Baltimore, MD.
- [39] A. E. Kaplan and P. L. Shkolnikov, "Theory of a superdriven two-level atom: very high harmonic generation and super-resonances", QELS'93, May 2-7, 1993, Baltimore, MD.
- [40] A. E. Kaplan and P. L. Shkolnikov, "Super-dressed two-level atom", International Conference on Multiphoton Processes (ICOMP VI), June 25-30, 1993, Quebec-City, Canada.
- [41] A. E. Kaplan and P. L. Shkolnikov, "Superdriven two-level atom: very high order harmonics and combination frequencies generation", Gordon Research Conference on Nonlinear Optics and Lasers, August 1-6, 1993, Wolfeboro, NH.
- [42] P. L. Shkolnikov, A. E. Kaplan, and A. Lago "Phase matching for high-order frequency upconversion", Gordon Research Conference on Nonlinear Optics and Lasers, August 1-6, 1993, Wolfeboro, NH.
- [43] A. E. Kaplan and P. L. Shkolnikov, "Superdriven two-level atom: very high order harmonic and combination frequency generation", OSA Annual/ILS-IX, October 3-8, 1993, Toronto, Canada.
- [44] A. E. Kaplan and P. L. Shkolnikov, "Super-dressed two-level atom: very high order harmonic generation and related phenomena" (*invited*), LEOS'93, November 15-19, 1993, San Jose, CA.
- [45] P. L. Shkolnikov, A. E. Kaplan and A. Lago, "Phase-matching optima for high-order multiwave mixing and harmonics generation beyond perturbation limits", Ultrafast Phenomena, 9-th Intern. Meeting, May 2-6, 1994, Dana Point, CA.
- [46] P. L. Shkolnikov and A. E. Kaplan, "X-ray nonlinear optics with high-order harmonics: frequency near-doubling", 4-th Int. Colloquium on X-ray Lasers, May 16-20, 1994, Williamsburg, MD.
- [47] P. L. Shkolnikov and A. E. Kaplan, "X-ray + optical mixings in plasma", 4-th Int. Colloquium on X-ray Lasers, May 16-20, 1994, Williamsburg, MD.
- [48] P. L. Shkolnikov, A. Lago and A. E. Kaplan, "Optimal quasi-phase-matching for high-order harmonics generation in gases and plasma", High Field Interactions and Short Wavelength Generation Topical Meeting, St. Malo, France, Aug. 21-25, 1994.
- [49] A. E. Kaplan, "Sub-Femtosecond Pulses in CSRS", High Field Interactions and Short Wavelength Generation Topical Meeting, St. Malo, France, Aug. 21-25, 1994.
- [50] A. E. Kaplan, "Sub-Femtosecond Pulses in mode-locked 2π solitons in CSRS", OSA/ILS'94 Annual Meeting (post-deadline paper), Oct. 2-7, 1994, Dallas, TX.

- [51] A. E. Kaplan and E. Hudis, "Modulation-induced inhibition of dynamics and high-order frequency mixing in a two-level atomic system", OSA/ILS'94 Annual Meeting (post-deadline paper), Oct. 2-7, 1994, Dallas, TX.
- [52] A. E. Kaplan, "Sub-Femtosecond Pulses in the Cascade Stimulated Raman Scattering" LEOS'94, Oct. 31 - Nov. 3, 1994, Boston, MA. (*invited*).
- [53] A. E. Kaplan, "Novel transient effects in two-level systems" (*invited*), Intern. Workshop on Laser Physics, Transient Coherent Phenomena, Oct. 10-14, 1994, New York, NY.
- [54] A. E. Kaplan and P. L. Shkolnikov, "Sub-femtosecond pulses in 2π solitons of the cascade stimulated Raman scattering" Nonlinear Guided Waves and Their Applications Topical Meeting, February 23-25, 1995, Dana Point, CA.
- [55] A. E. Kaplan and P. L. Shkolnikov, "No-carrier high-intensity subfemtosecond solitons", Quantum Electronics and Laser Science Conference, May 21-26, 1995, Baltimore, MD.
- [56] A. E. Kaplan and E. Hudis, "Modulation-Induced Multi-transparency and high order frequency mixing in a two-level atomic system", QELS Conf., May 21-26, 1995, Baltimore, MD.
- [57] A. E. Kaplan and P. L. Shkolnikov, "Electromagnetic bubbles': unipolar (non-oscillatory) solitons", 1995 OSA Annual Meeting, September 10-15, 1995, Portland, OR.
- [58] A. E. Kaplan and P. L. Shkolnikov, "Laser super-gate for electron beams", 1995 OSA Annual Meeting, September 10-15, 1995, Portland, OR.
- [59] A. E. Kaplan and Y. J. Ding, "Field-gradient induced second harmonic generation in magnetized vacuum", 1995 OSA Annual Meeting, September 10-15, 1995, Portland, OR.
- [60] * A. E. Kaplan, "On the road to high-intensity subpicosecond pulses" (* *invited talk*), Intern. Conf. on Nonlinear Optics, May 28 - June 2 1995, Calabria, Italy.